People`s Democratic Republic of Algeria
Ministry of Higher Education and Scientific Research
University of Echahid Hamma Lakhdar - El Oued
Faculty of Technology
Department of Process Engineering & Petrochemistry

Dissertation

ACADEMIC MASTER

Domain: Science and Technology

Division: Telecommunications

Specialty: Telecommunications Systems

Presented by:

1. **Soufia Abdelhafid**
2. **Soufia Raid Abdelhafid**

Entitled:

Numerical simulation study of solar cell

Dissertation Submitted in Partial Fulfillment of the Requirements for the Master Degree in Telecommunications Systems

Board of Examiners:

Dr. MOUSSI Fouaze	**Chairman**
Dr. KATEB Mohamed Nadjib	**Supervisor**
Dr. BELLILI Nour Elimane	**Examiner**

Academic Year: 2024/2025

Abstract

A numerical simulation study of solar cells employs computational techniques to model and analyse the behaviour of solar cells under various operating conditions. By solving physical equations governing charge carrier transport, light absorption, and electrical performance, these simulations provide valuable insights into the internal mechanisms of solar cells. The approach enables the optimization of design parameters, such as material properties, layer thickness, and doping concentration, to maximize efficiency. Furthermore, numerical simulations allow for the prediction of solar cell performance, offering a cost-effective and time-efficient alternative to experimental trial-and-error methods. This study emphasizes the importance of numerical simulations in advancing solar cell technology and accelerating the development of high-performance photovoltaic devices.

ملخص

تستخدم دراسة محاكاة عددية للخلايا الشمسية تقنيات حسابية لنمذجة وتحليل سلوكها في ظل ظروف تشغيل متنوعة. ومن خلال حل المعادلات الفيزيائية التي تحكم نقل حاملات الشحنة، وامتصاص الضوء، والأداء الكهربائي، توفر هذه المحاكاة رؤى قيّمة حول الآليات الداخلية للخلايا الشمسية. ويتيح هذا النهج تحسين معايير التصميم، مثل خصائص المادة، وسمك الطبقة، وتركيز التشويب، لتحقيق أقصى قدر من الكفاءة. علاوة على ذلك، تتيح المحاكاة العددية التنبؤ بأداء الخلايا الشمسية، مما يوفر بديلاً فعالاً من حيث التكلفة والوقت لأساليب التجربة والخطأ التجريبية. وتؤكد هذه الدراسة على أهمية المحاكاة العددية في تطوير تكنولوجيا الخلايا الشمسية وتسريع تطوير الأجهزة الكهروضوئية عالية الأداء.

Dedication

To our dear parents,

who have always been a source of strength and support, and who never hesitated to offer me advice and guidance. we extend my deepest gratitude for the love and care you have given us,

as you were the foundation upon which this success was built.

To our esteemed teachers,

who generously shared their knowledge and experience, and continuously guided us in the right direction. Thank you for your unwavering support, belief in our abilities, and motivating

we to strive for excellence.

To our dear friends,

who stood by our side at every step, never hesitating to offer help and encouragement. Thank you for always being there, as your support was a driving force in overcoming challenges and

achieving this accomplishment.

And finally, to us ,

for being patient and persistent, and for not giving up despite the hardships. we dedicate this

success to us and take pride in what we have achieved.

Thanks, and Appreciation

All praise and gratitude are due to God for granting us the strength and success to complete this work.

We are deeply thankful to everyone who supported us throughout our academic journey.

we extend our heartfelt appreciation to our esteemed professors for their generosity in sharing knowledge and offering invaluable guidance. Their insights greatly enriched our understanding

and played a vital role in the development of this research. We are truly grateful for their time,

effort, and patience.

our deepest gratitude goes to our beloved parents, whose unwavering support—both emotional

and financial—has been the foundation of my progress. Their constant presence and encouragement have been the driving force behind this achievement.

We are also thankful to our friends and colleagues who accompanied us on this journey, offering

consistent support and motivation along the way.

Lastly, we would like to thank everyone who contributed, directly or indirectly, to the completion

of this dissertation. we hope that the final outcome meets the expectations of all who have

supported us.

TABLE OF CONTENTS

LIST OF FIGURES

Chapter 1: Electronic properties of semiconductor materials

Chapter 2: Solar cells fundamentals device

Chapter 3: SCAPS-1D program and simulation

LIST OF TABLES

Chapter 1: Electronic properties of semiconductor materials

Chapter 3: SCAPS-1D program and simulation

General introduction

The pursuit of efficient and sustainable energy sources has led to significant advancements in photovoltaic technology, with a particular focus on materials that can optimize solar energy conversion. Among these, indium gallium phosphide (InGaP) has emerged as a promising material due to its excellent optical and electrical properties, making it a key candidate for high-efficiency solar cells, especially in tandem configurations. This work explores the fundamentals of solar cells, with a primary focus on the simulation and optimization of InGaP-based devices using the SCAPS-1D simulation software.

Chapter 1 introduces the basics of solar cell technology, discussing the fundamental principles of photovoltaic physics, including the photovoltaic effect, charge carrier generation and recombination, and the role of different materials in solar cells. It provides an overview of the types of materials used in solar cells, from silicon to III-V semiconductors, and highlights the growing interest in multi-junction cells, where materials like InGaP play a critical role.

Chapter 2 dives deeper into the simulation and optimization process for InGaP-based solar cells, focusing on the use of SCAPS-1D, a powerful simulation tool for modeling the electrical and optical behavior of thin-film solar cells. This chapter details the numerical techniques employed in SCAPS, including solving key semiconductor equations and the software's ability to simulate various types of solar cell structures. It also discusses the importance of optimizing device parameters such as layer thickness and doping concentrations to maximize solar cell efficiency.

Finally, Chapter 3 presents the results of simulations conducted on InGaP and InGaP/Ge solar cells. By adjusting key parameters such as layer thickness and doping concentrations, we achieved notable improvements in solar cell efficiency. The chapter provides a detailed analysis of the photovoltaic parameters for both the single-junction InGaP cell and the tandem InGaP/Ge cell, highlighting the potential of InGaP-based devices for high-efficiency solar applications. Through these simulations, we demonstrate the critical role of optimization in enhancing the performance of solar cells and the utility of SCAPS-1D in photovoltaic research.

Together, these chapters outline the theoretical foundation, simulation methodology, and practical outcomes of optimizing InGaP-based solar cells, contributing to the broader effort to advance solar energy technology.

Chapter 1:
Electronic properties of semiconductor materials

1.1 Introduction

Semiconductor materials play a central role in modern technology, particularly in the manufacturing of electronic devices such as transistors, diodes, and photovoltaic cells. Their most distinctive property lies in their ability to conduct electricity in a manner that is intermediate between conductors and insulators. This conductivity can be finely tuned by modifying parameters such as temperature, chemical composition, or the introduction of impurities (doping). The Electronic properties of semiconductors, such as the bandgap width, charge carrier mobility, and electronic state density, determine their behavior in practical applications. This introduction aims to explore the fundamental characteristics of semiconductors and their crucial role in contemporary technological advancements.

1.2 Crystal structure

Semiconductors exhibit a highly ordered and periodic arrangement of atoms in a crystal lattice. The most common crystal structures found in semiconductors are:

- Diamond cubic structure (silicon, germanium)
- Zinc blende structure (gallium arsenide, indium phosphide)
- Wurtzite structure (gallium nitride, zinc oxide)

The cubic structure of diamond consists of two interpenetrating face-centered cubic (FCC) lattices, with each atom bonded to four nearest neighbors in a tetrahedral arrangement. The zincblende structure is similar to the cubic structure of diamond but with alternating types of atoms (for example, gallium and arsenic) occupying the lattice sites. The wurtzite structure has a hexagonal unit cell, with each atom bonded to four nearest neighbors in a tetrahedral arrangement. The crystal structure determines the symmetry, lattice constants, and electronic properties of the semiconductor. Defects and impurities in the crystal structure can have a significant impact on the electrical and optical properties of the semiconductor [1,2].

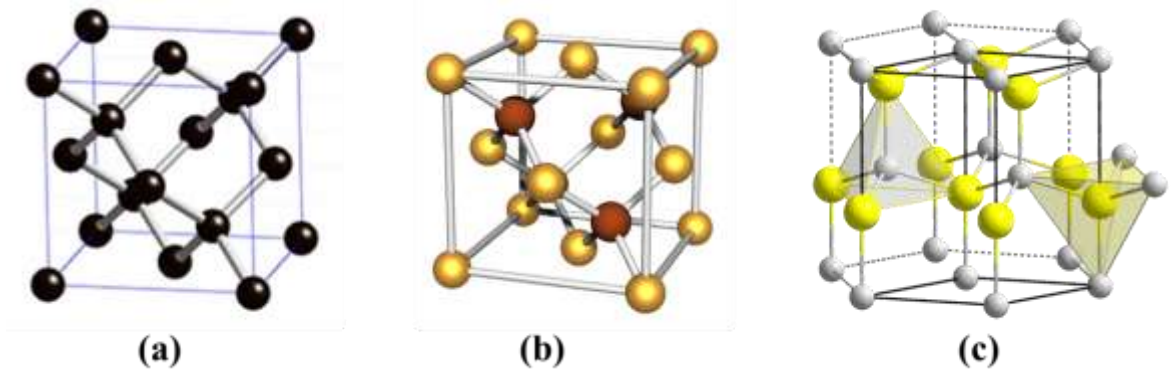

Figure 1.1 (a) Diamond lattice, (b) Zinc blende lattice, (c) Wurtzite structure

1.3 Semiconductor Materials

Semiconductor materials belong to different groups of the periodic table but share certain similarities.

The properties of semiconductor materials are related to their atomic characteristics and vary from one group to another. Researchers and designers take advantage of these differences to improve design and choose the optimal material for a photovoltaic application.

Periode	Column II	III	IV	V	VI
2		B	C	N	O
3	Mg	Al	Si	P	S
4	Zn	Ga	Ge	As	Se
5	Cd	In	Sn	Sb	Te
6	Hg		Pd		

Table 1.1 Portion periodic table related to semiconductors.

The semi-conductor parts are on the mats of group IV on the periodic table, or the combination of group III and group V (appel semi-conductors III-V), or the combinations of group II and group VI (appel semi-conductors II-VI). Don't forget that the different semi-conductors are located in different groups of different semi-conductors at the end of the table. The silicium, which belongs to Group IV, is the semi-conductor mat for the most common car use and is based on the base of integrated circuits (CI) and the most mature technology and the solar cell parts are based on the silicium base. A semiconductor can be either a single element, such as Si or Ge, or a compound, such as GaAs, InP, or CdTe, or an alloy, such as SixGe(1-x) or AlxGa(1-x)As, where x is the fraction of the particular element and ranges from 0 to 1 [3].

1.4 Properties and Applications

Semiconductors exhibit unique electrical and optical properties that make them essential for modern electronic devices.

Electrical properties:

- Controllable electrical conductivity through doping and external factors (temperature, electric field).

- Ability to form p-n junctions, which are the basic building blocks of diodes and transistors.
- High mobility of electrons and holes, allowing for fast switching and high-frequency operation.

Optical properties:

- Absorption and emission of light at specific wavelengths determined by the bandgap.
- Photovoltaic effect, enabling the conversion of light into electrical energy (solar cells).
- Electroluminescence, allowing for the emission of light from semiconductors (LEDs).

Semiconductors find extensive applications in various fields, including:

- Electronics: Transistors, integrated circuits, memory devices, power electronics.
- Optoelectronics: LEDs, laser diodes, photodetectors, solar cells.
- Sensors: Temperature sensors, pressure sensors, chemical sensors
- Energy production: Solar panels, thermoelectric generators.

The continuous advancement of semiconductor technology has revolutionized modern electronics and paved the way for miniaturization, high-performance computing, and energy-efficient devices [2].

1.5 Energy bands

In gaseous substances, the arrangement of molecules is dispersed, and they are not very close to each other. In liquids, the molecules are closer to one another. However, in solids, the molecules are tightly packed together, causing the atoms of the molecules to tend to move into the orbitals of neighboring atoms. Consequently, the electronic orbitals overlap when the atoms come closer.

1.5.1 Classification of energy bands

a) Valence band:

The electrons in the outermost shell are called valence electrons. These valence electrons contain a series of energy levels and form an energy band called the valence band. The valence band has the highest occupied energy level.

b) Conduction band:

Valence electrons are not tightly bound to the nucleus, which causes some of these valence electrons to leave the outermost orbit even at room temperature and become free electrons. Free electrons conduct current in conductors and are therefore called conduction electrons. The

conduction band is the one that contains conduction electrons and has the lowest occupied energy levels.

c) Forbidden energy gap:

The gap between the valence band and the conduction band is called the forbidden gap. As its name suggests, the forbidden gap has no energy, and no electron remains in this band. If the forbidden energy gap is larger, then the electrons in the valence band are tightly bound or firmly attached to the nucleus. We need a certain amount of external energy equal to the forbidden energy gap [4].

1.6 Conduction in metals, semiconductors, and insulators

The enormous variation in electrical conductivity of metals, semiconductors, and insulators may be explained qualitatively in terms of their energy bands. Figure 1.2 shows the energy band diagrams of three classes of solids: metals, semiconductors, and insulators.

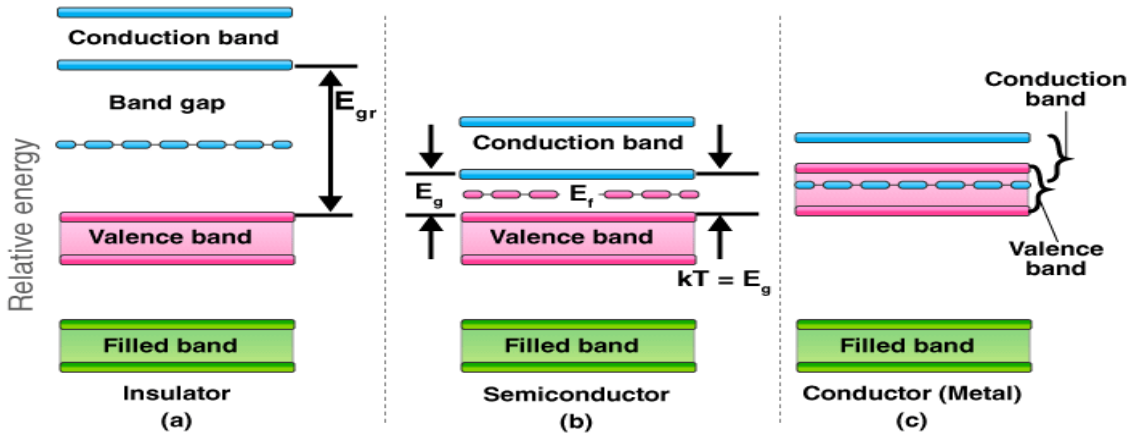

Figure 1.2 Schematic energy band representations of (a) an insulator, (b) a semiconductor, (c). a conductor.

1.6.a Metals

The characteristics of a metal (also called a conductor) include a very low value of resistivity and a conduction band that either is partially filled (as in Cu) or overlaps the valence band (as in Zn or Pb) so that there is no bandgap, as shown in Fig. 1.3(a). As a consequence, the uppermost electrons in the partially filled band or electrons at the top of the valence band can move to the next higher available energy level when they gain kinetic energy (e.g., from an applied electric field). Electrons are free to move with only a small applied field in a metal

because there are many unoccupied states close to the occupied energy states. Therefore, current conduction can readily occur in conductors.

1.6.b Semiconductors

Now, consider a material that has a much smaller energy gap, on the order of 1 eV (Fig. 1.3(b)). Such materials are called semiconductors. At $T = 0$ K, all electrons are in the valence band, and there are no electrons in the conduction band. Thus, semiconductors are poor conductors at low temperatures. At room temperature and under normal atmospheres, values of E_g are 1.12 eV for Si and 1.42 eV for GaAs. At room temperature, appreciable numbers of electrons are thermally excited from the valence band to the conduction band. Since there are many empty states in the conduction band, a small applied potential can easily move these electrons, resulting in a moderate current.

1.6.c Insulators

In an insulator such as silicon dioxide (SiO_2), the valence electrons form strong bonds between neighboring atoms. Since these bonds are difficult to break, there are no free electrons to participate in current conduction at or near room temperature. As shown in the energy band diagram (Fig. 1.3(c)), insulators are characterized by a large bandgap. Note that electrons occupy all energy levels in the valence band and all energy levels in the conduction band are empty. Thermal energy or the energy of an applied electric field is insufficient to raise the uppermost electron in the valence band to the conduction band. Thus, although an insulator has many vacant states in the conduction band that can accept electrons, so few electrons actually occupy conduction band states that the overall contribution to electrical conductivity is very small, resulting in a very high resistivity. Therefore, silicon dioxide is an insulator; it cannot conduct current [5].

Material	Eg(eV)	Note
C	**5.5**	**Insolent T=300K**
Si	**1.12**	**Semiconductor T=300K**
Ge	**0.76**	**Semiconductor T=300K**

Table 1.2 Examples: Energy gap Eg of carbon, silicon, and germanium (minimum energy required to create an electron-hole pair. [6])

1.7 Intrinsic semiconductors

Intrinsic semiconductors contain no (in practice, very few) impurities compared with the number of thermally generated electrons and holes. For this condition we shall attempt to estimate the number of free charge carriers (electrons and holes) under equilibrium conditions. The occupation probability for an electronic state is given by the Fermi-Dirac function

$$f(E) = \frac{1}{1+\exp((E - E_F)/(k_B T))} \tag{1.1}$$

Where E_F, the Fermi energy, is the energy at which the occupation probability of a (possible) state is one half, k is the Boltzmann constant and T is the absolute temperature [1,7].

The density of free electrons n is obtained by integrating the carrier concentration (Fig. 1.3(d)) given by the product of the density of states N (Fig. 1.3(b)) and the occupation probability $F_n(E)$ (Fig. 1.3(c)) over the conduction band:

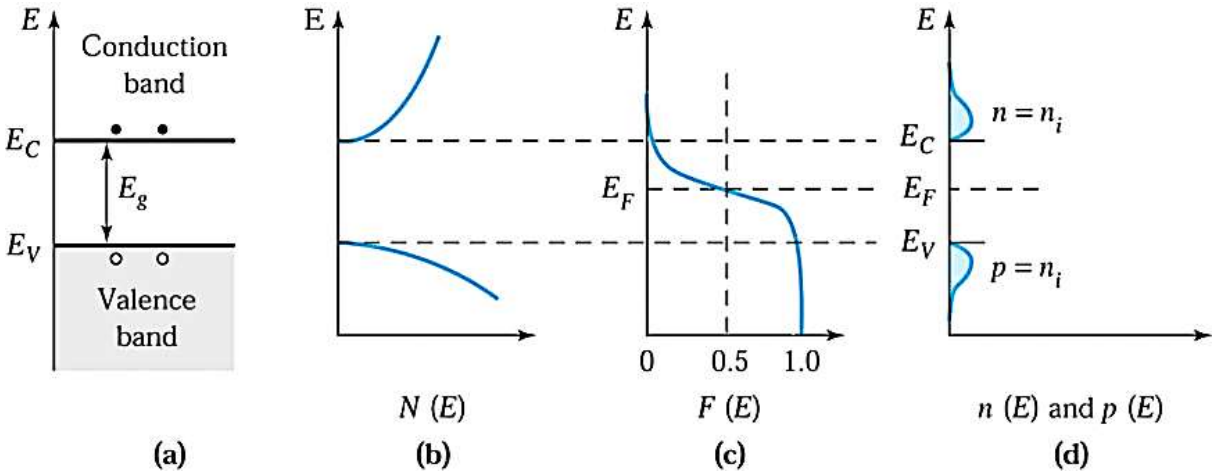

Figure 1.3 Intrinsic semiconductor: (a) Schematic band diagram, (b) Density of states, (c) Fermi distribution function, (d) Carrier concentration.

$$n = 2\left(\frac{2\pi m_n kT}{h^2}\right)^{\frac{3}{2}} e^{-\frac{E_C - E_F}{kT}} = N_C e^{-\frac{E_C - E_F}{kT}} \tag{1.2(a)}$$

Similarily for holes, we have:

$$p = 2\left(\frac{2\pi m_p kT}{h^2}\right)^{\frac{3}{2}} e^{-\frac{E_F - E_V}{kT}} = N_C e^{-\frac{E_F - E_V}{kT}} \tag{1.2(b)}$$

N_C and N_V are the effective densities of states in the conduction and valence bands respectively. The product of electron and hole concentration, given by $n.p = N_C N_V e^{-\frac{E_C - E_V}{kT}}$, depends on the band gap $E_G = E_C - E_V$ and is thus independent of the Fermi level E_F.

So far the value of the Fermi level E_F has not been specified and equations (1.1) to (1.2) will also be valid for extrinsic semiconductors (to be dealt with in the following chapter). The Fermi level for intrinsic semiconductors E_i can be found from the requirement that the numbers of electrons and holes are equal*:* $n = p = n_i$. One thus finds that:

$$n_i = \sqrt{N_C N_V}\, e^{-\frac{E_C - E_V}{2kT}} = \sqrt{N_C N_V}\, e^{-\frac{E_G}{2kT}} \tag{1.3}$$

And

$$E_i = \frac{E_C + E_V}{2} + \frac{3kT}{4} \ln\left(\frac{m_p}{m_n}\right) \tag{1.4}$$

where E_i is the Fermi level close to the middle of the band gap, the deviation being due to the unequal effective masses of electrons and holes.

Introducing the intrinsic carrier density n_i and the intrinsic level E_i, one may reformulate the more generally valid (1.2) in the useful form:

$$n = n_i e^{\frac{E_F - E_i}{kT}} \qquad p = n_i e^{\frac{E_i - E_F}{kT}} \tag{1.5}$$

1.8 Extrinsic semiconductors

Intrinsic semiconductors are rarely used in semiconductor devices since it is extremely difficult to obtain sufficient purity in the material. Moreover, in most cases one intentionally alters the property of the material by adding small fractions of specific impurities. This procedure, which can be performed either during crystal growth or later in selected regions of the crystal, is called doping. Depending on the type of added material, one obtains n-type semiconductors with an excess of electrons in the conduction band or p-type with additional holes in the valence band. We will look at extrinsic semiconductors through the simple bond representation and also through a band model.

Figure 1.4(a) shows a two-dimensional schematic bond representation of a silicon crystal with one silicon atom replaced by an arsenic atom with five valence electrons. Only four are used for the formation of covalent bonds with neighboring atoms, while the fifth is not

bound to a specific atom but is free for conduction. It should be stressed that the crystal as a whole remains uncharged, since the charge of the free electron is compensated for by the excess charge of the arsenic nucleus bound in the crystal lattice.

If a silicon atom is replaced by an atom with only three valence electrons (Fig. 1.4(b)) one electron is missing in the covalent bonds and a hole is thus created. This hole may be filled by an electron from a neighboring atom, this being equivalent to a movement of the hole. The hole is free for conduction. (That the moving hole is more than a missing electron whose place is filled by a neighboring electron follows from quantum mechanical considerations and is experimentally verified in the Hall experiment) [1,7].

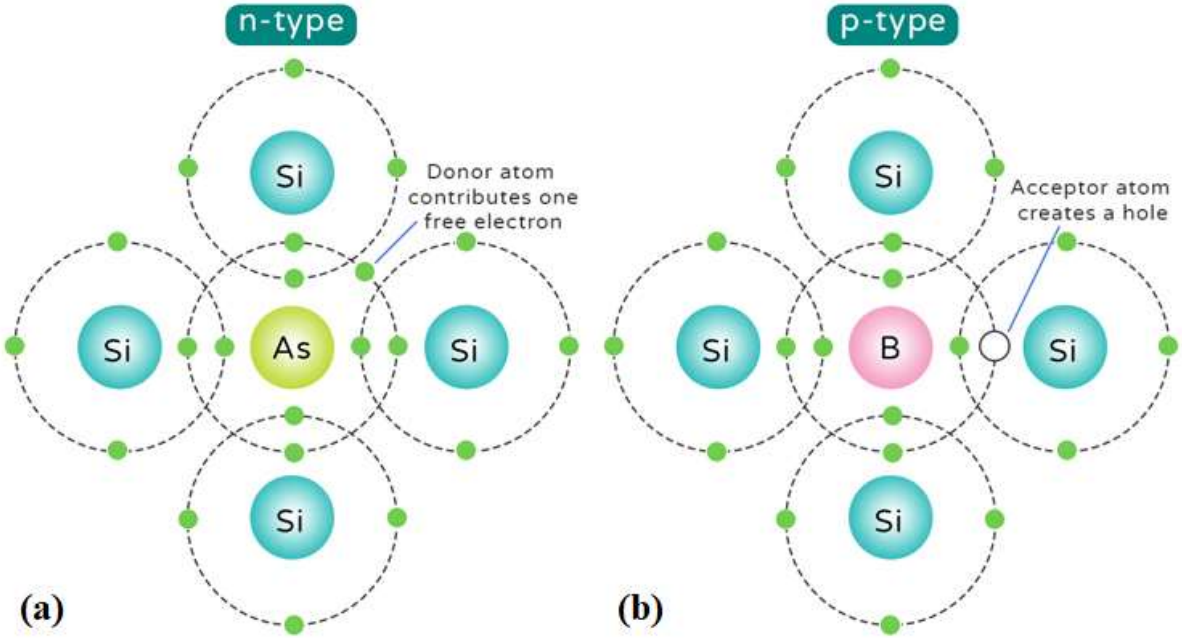

Figure 1.4 Schematic bond pictures for (a) n-type Si with donor (arsenic) and (b) p-type Si with acceptor (boron).

The replacement of a proper atom of the lattice by a different atom is accompanied by the creation of localized energy levels in the band gap. These energy levels may be of the donor (E_D) or acceptor (E_A) type. If donor levels E_D are close to the conduction band, as is the case for phosphorous ($E_C - E_D$ = 0.045 eV) or arsenic ($E_C - E_D$ = 0.054 eV) atoms in silicon, for instance, these states will be almost completely ionized at room temperature and the electrons will be transported to the conduction band (Fig. 1.5(a)). This is due to the many states with

similar energy level nearby in the conduction band, with which the donor states have to share their electrons.

Equivalent considerations hold for acceptor-type states, e.g. boron in silicon ($E_A - E_V$ = 0.045 eV). These states will be filled almost completely and holes will be created in the valence band (Fig. 1.5(b)) [1,7].

The situation that the donor levels are almost completely ionized can be described by a movement of the Fermi level E_F from the intrinsic level E_i towards the conduction band.

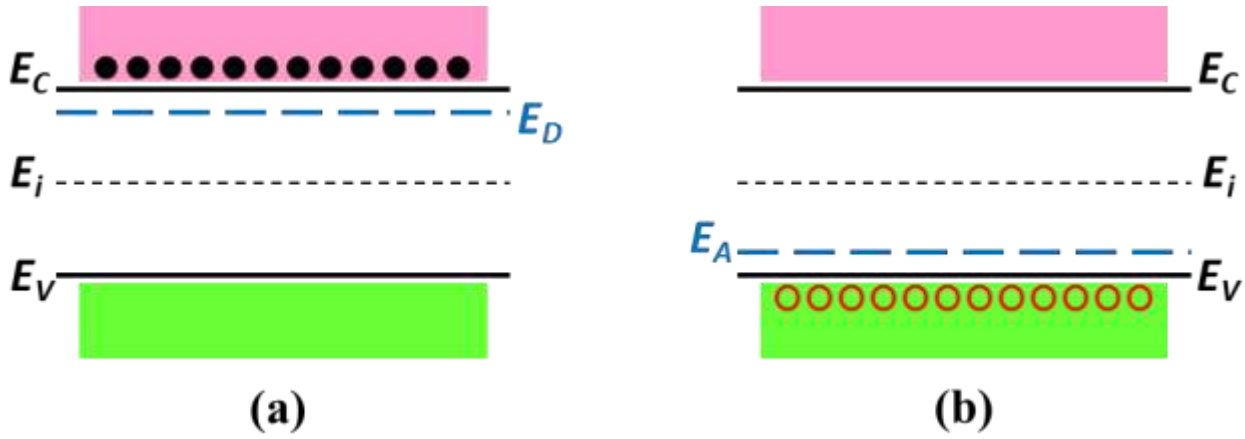

Figure 1.5 (a) Schematic energy band representation of extrinsic n-type, (b) p-type semiconductors.

By setting the electron concentration in the conduction band n equal to the donor concentration N_D, thus:

$$E_C - E_F = kT \ln \frac{N_C}{N_D} \tag{1.6}$$

Similarly, one obtains for p-type material and acceptor concentration N_A:

$$E_F - E_V = kT \ln \frac{N_V}{N_A} \tag{1.7}$$

A somewhat more complicated treatment is required for the simultaneous presence of donors and acceptors and for very high doping concentrations. It may also be mentioned in this context that the number of donor or acceptor states does not necessarily equal the number of corresponding impurity atoms, since in order to become electrically active doping atoms they have to be properly built into the crystal lattice [1,7].

The density of free electrons *n* is

$$n = n_i e^{\frac{E_F - E_i}{kT}} \tag{1.8(a)}$$

The density of free holes *p* is

$$p = n_i e^{\frac{E_i - E_F}{kT}} \tag{1.8(b)}$$

The increase of majority carriers (electrons in the case of n-type material) is accompanied by a decrease of minority carriers according to the mass-action law

$$n.p = n_i^2 \tag{1.9}$$

In agreement with (1.8) [1,7].

1.9 Electron and hole current

In conductor current is caused by only motion of electrons but in semiconductors current is caused by both electrons in band and conduction holes in valence band. Current that is caused by electron motion is called electron current and current that is caused by hole motion is called hole current. Electron is a negative charge carrier whereas hole is a positive charge carrier. At absolute zero temperature intrinsic semiconductor behaves as insulator. However, at room temperature the electrons present in the outermost orbit absorb thermal energy. When the outermost orbit electrons get enough energy then they will break bonding with the nucleus of atom and jumps in to conduction band. The electrons present in conduction band are not attached to the nucleus of an atom so they are free to move. When the valence electron moves from valence band to the conduction band a vacancy is created in the valence band where electron left. Such vacancy is called hole.

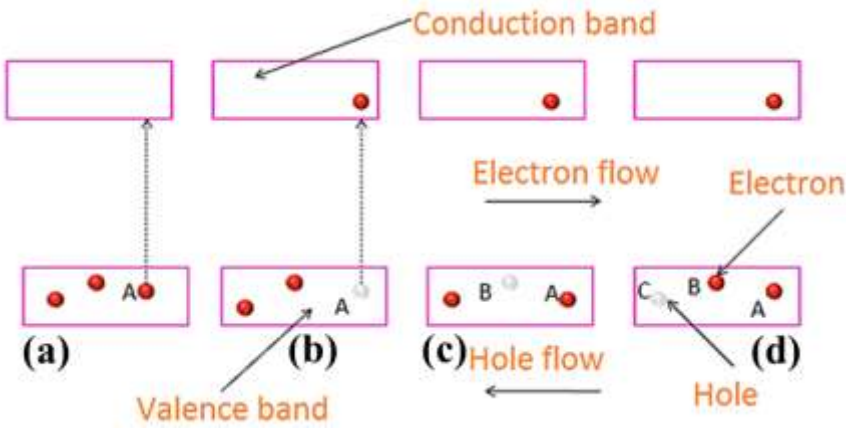

Figure 1.6 Electron and hole current

Let's take an example, as shown in fig there are three atoms atom A, atom B and atom C. At room temperature valence electron in an atom A gains enough energy and jumps in to conduction band as show in fig (1.16.a). When it jumps in to conduction band a hole (vacancy) is created in the valence band at atom A as show in fig (1.16.b). Then, the neighboring electron from atom B moves to atom A to fill the hole at atom A. This creates a hole at atom B as show in fig (1.16.c). Similarly neighboring electron from atom C moves to atom B to fill the hole at atom B. This creates a hole at atom C as show in fig (1.16.d). Likewise, electrons move from left side to right side and holes moves from right to left side [8].

1.10 Currents in the Semiconductor

The currents in the semiconductor result from the movement of charge carriers, electrons, and holes, under the influence of different forces. The origin of these forces can be an electric field (conduction current) or a concentration gradient (diffusion current) [4].
The conduction current for each type of carrier (electrons, holes) is due to the electric field:

$$\overrightarrow{j_n} = en\mu_n \overrightarrow{E} \tag{1.9}$$

$$\overrightarrow{j_p} = ep\mu_p \overrightarrow{E} \tag{1.10}$$

The total current is then written as:

$$\overrightarrow{J_c} = e(n\mu_n + p\mu_p)\,\overrightarrow{E} = \sigma \overrightarrow{E} \tag{1.11}$$

With $\sigma = e(n\mu_n + p\mu_p)$ being the conductivity and $\mu_n(\mu_p)$ being the mobility of the electrons (holes).

When the free carriers are not uniformly distributed in the semiconductor, they undergo the diffusion process. The movement of charge carriers corresponds to diffusion currents:

$$\overrightarrow{j_{dn}} = eD_n \frac{dn}{dx} \tag{1.12}$$

$$\overrightarrow{j_{dp}} = -eD_p \frac{dp}{dx} \tag{1.13}$$

D_n and D_p are the diffusion constants of electrons and holes, respectively. The total diffusion current is then written as:

$$\overrightarrow{j_d} = eD_n \frac{dn}{dx} - eD_p \frac{dp}{dx} \tag{1.14}$$

Considering expressions (1.9), (1.10), and (1.12), (1.13), the resulting currents of electrons and holes are written as:

$$\overrightarrow{j_n} = e\mu_n n\overrightarrow{E} + eD_n \frac{dn}{dx} \tag{1.15.a}$$

$$\overrightarrow{j_p} = e\mu_p p\overrightarrow{E} - eD_p \frac{dp}{dx} \tag{1.15.b}$$

The diffusion constant D and the mobility μ of a type of carrier are related by the Einstein relation [9]:

$$\frac{D_n}{\mu_n} = \frac{D_p}{\mu_p} = \frac{KT}{e} \tag{1.16}$$

1.11 generation and recombination

The free electron and hole concentrations in bulk semiconductors can be modified by the processes of generation and recombination, and also by the transport of electrons and holes through drift and diffusion. Generation: e.g., absorption of a photon generates a free electron and a free hole (an electron-hole pair).

Recombination: can be radiative, in which case a photon is emitted as the electron returns to the valence band, or non-radiative, in which case the energy associated with the e-h pair is converted to heat, or transferred to another charge carrier (Auger recombination) – non-radiative corresponds to no photon.

Transport is the movement of charge carriers under forces based either on an electric field, or on a concentration gradient:

Drift refers to the motion of charge carriers under the force of an electric field. Motion is typically not “ballistic”, and instead includes the resistive action of scattering.

Diffusion refers to motion of electron and holes due to the presence of a concentration gradient. Charge carriers move between valence and conduction bands under thermal influence (thermal excitation within the Boltzmann tail of the Fermi-Dirac distribution).

In the dark and at equilibrium, the concentration of electrons and holes are unaffected by these processes.

-Generation, under influence of light absorption for example, promotes electrons from the valence band to the conduction band, resulting in a new free electron in the CB, and a new hole in the VB.

- Recombination is essentially the reverse process, in which an electron returns to the valence band, giving up it electronic potential energy to a photon, or a third carrier, or to phonons [10].

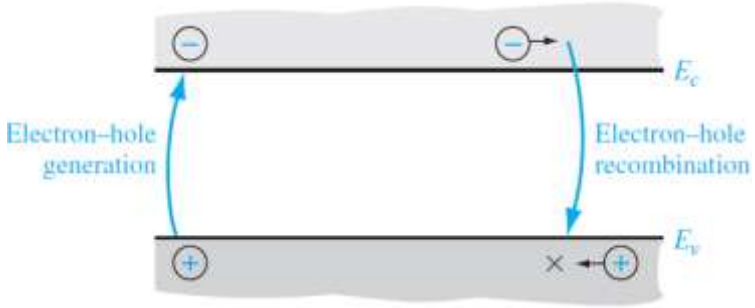

Figure 1.7 Electron-hole generation and recombination

1.12 InGaP

Ingap is a hybrid semiconductor composed of indium, gallium, and phosphorus, also known as Indium gallium phosphide (InGaP) or gallium indium phosphide (GaInP). It has a large bandgap and excellent etch selectivity. InGaP with lattice matched to GaAs is commonly used in high-power and high-frequency devices, such as InGaP/gallium arsenide (GaAs) heterojunction bipolar transistor (InGaP-HBT) power amplifiers (PAs) in mobile communications and wireless network terminals [11].

1.13 Conclusion

This chapter provides a comprehensive overview of semiconductor materials, highlighting their unique ability to control electrical conductivity. It explains the role of crystal structures and periodic table groupings in defining semiconductor properties. The chapter covers intrinsic and extrinsic semiconductors, energy bands, and current flow through electrons and holes. It also explores electrical and optical behaviors, including conduction, diffusion, generation, and recombination. These foundational concepts underscore the critical role of semiconductors in modern electronic and optoelectronic applications.

Chapter 1 references

[1] G. Lutz, Semiconductor radiation detectors. Springer, 2007.

[2] Fiveable.com

[3] www.pveducation.org

[4] byjus.com

[5] https://ensah.netlify.app/

[6] S. M. Sze and M. K. Lee, “Semiconductor devices: phys-ics and technology. 3-rd edition. -New York, John Wiley and Sons, Inc,” 2012.

[7] Amina, A., & Anhar, C. (2024). *Optimization of solar cell performance through numerical simulation* [Master Thesis]. University of Echahid Hamma Lakhdar - El Oued.

[8] Electron and Hole Current in Semiconductor. (2025). In ddugu. http://ddugu.ac.in/ePathshala_Attachments/STUDY170@633182.pdf

[9] H. Mathieu, "Physique des semiconducteurs et des composants électroniques", 2ème Edition, Masson, 1990.

[10] GENERATION AND RECOMBINATION OF CHARGE CARRIERS IN SOLAR CELLS; TRANSPORT MECHANISMS: DRIFT AND DIFFUSION. (2012). In University of Toledo.

[11] https://taylorandfrancis.com/

Chapter 2:

Solar cells fundamentals device

2.1 intrudoction

Solar cells, also known as photovoltaic (PV) cells, are at the heart of solar energy technology. They are devices that convert sunlight directly into electricity using the photovoltaic effect, a process that transforms light energy into electrical energy. As the world increasingly shifts toward renewable energy sources, solar cells have become a critical technology for harnessing the sun's abundant and clean energy. This chapter provides an introduction to the fundamental principles and working mechanisms of solar cells. It explores the basic physics behind the photovoltaic effect, the materials used in solar cell construction, and the key components that make up a solar cell device. By understanding these fundamentals, we can appreciate how solar cells generate electricity and how they are designed to maximize efficiency and performance. The chapter also touches on the various types of solar cells, from traditional silicon-based cells to emerging technologies like thin-film and perovskite solar cells. Each type has its unique advantages and challenges, and ongoing research continues to push the boundaries of efficiency, cost-effectiveness, and sustainability. Whether you are new to the field or looking to deepen your understanding, this chapter serves as a foundation for exploring the exciting world of solar energy and its potential to power a sustainable future

2.2 solar radiation

Solar radiation, often called the solar resource or just sunlight, is a general term for the electromagnetic radiation emitted by the sun. Solar radiation can be captured and turned into useful forms of energy, such as heat and electricity, using a variety of technologies. However, the technical feasibility and economical operation of these technologies at a specific location depends on the available solar resource [1].

Figure 2.1 shows two curves related to solar spectral irradiance (power per unit area per unit wavelength). The upper curve, which represents the solar spectrum outside the Earth’s atmosphere, is the air mass zero condition (AM0). The AM0 spectrum is relevant for satellite and space vehicle applications. Terrestrial solar cell performance is specified with reference to the air mass 1.5 (AM 1.5) spectrum. This spectrum represents the sunlight at the Earth’s surface when the sun is at an angle of 48° from the vertical. At this angle the incident power is about 963 W/m² [2].

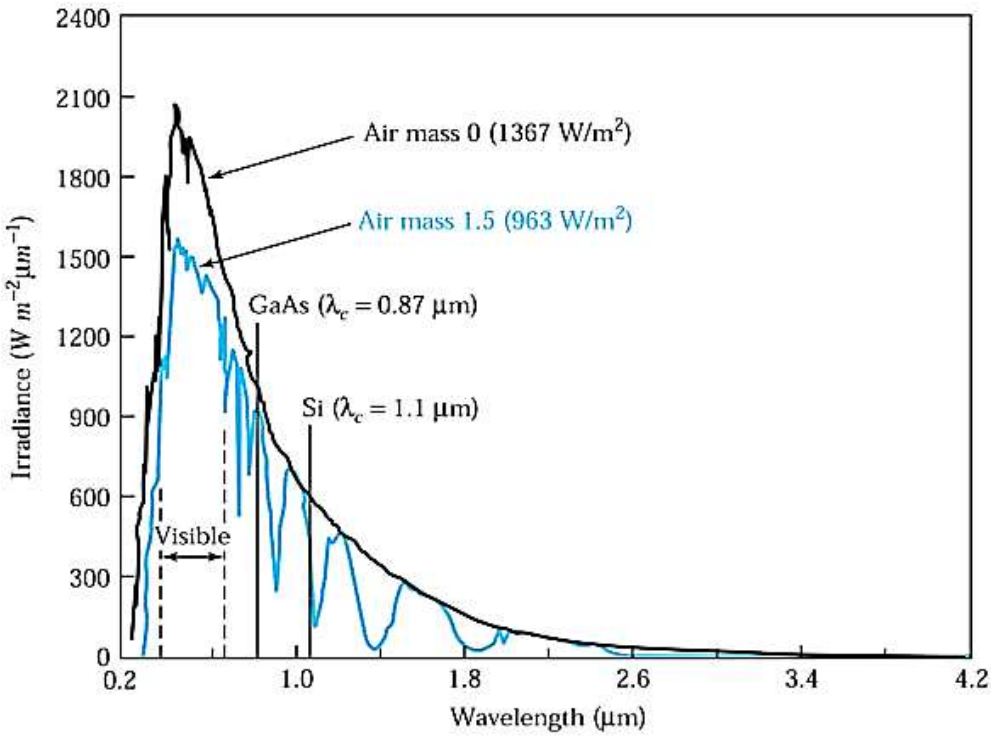

Figure 2.1 Solar spectral irradiance at air mass 0 and air mass 1.5 and the cutoff wavelength of GaAs and Si.

2.3 Transfer of energy from the photon to the electron

Sunlight acting as a fuel carries energy into the photovoltaic cell. When a photon particle from the sunlight strikes the surface of the silicon solar cell or the doped structures made up of silicon-phosphorus or silicon-boron, the photons of the absorbed sunlight knocks loose and dislodges electrons from the silicon atoms of the cell transferring the energy and exciting them. This excitation of the electrons causes them to become released from its parent atom and moves to a higher valance level. As there are billions of photons striking the cell every second, there are lots of electrons knocked loose.

Eventually, the excited electron gets kicked out of the atom allowing it to roam freely around the semiconductor material. As one side of the PN junction has a “lack of electrons” (holes) while the other side of the junction has an “excess of electrons” these free electrons move through the junction, creating and filling in holes in the cell.

It is this movement of electrons and holes that generates electricity and as long as there is light striking the cell, there will be electrons flowing out of the cell. The physical process in which a PV cell converts sunlight into electricity is known as the photovoltaic effect.

The electrons freed by the interaction of the sunlight with the semiconductor material creates an electron flow as the free electrons move together around an external circuit. The generation

of electrical power requires both voltage and current. So in order to produce power, the PV cell must generate voltage as well as the current provided by the flow of electrons [3].

2.4 Absorption of light

The energy of the photon corresponding to a given radiation is related to its wavelength by the relation [4]:

$$E_p = h\nu = \frac{hc}{\lambda} = \frac{1.24}{\lambda} \tag{2.1}$$

Photons interact with the semiconductor depending on their energy:

- *Ephoton* < *Eg* : Photons with energy below the band gap energy are transmitted through the material;
- *Ephoton* = *Eg* : These photons have sufficient energy to be absorbed in a band-to-band transition, and generate an electron-hole pair. Absorption of these photons will be relatively weak
- *Ephoton* > *Eg* : Photons with significantly greater energy than the semiconductors bandgap are relatively strongly absorbed, and generate electron-hole pairs with initial excess kinetic energy. This excess kinetic energy is, in general, quickly lost to the lattice as phonons).

The generation rate quantifies the number of electron-hole pairs created per unit time. As the light enters and travels through the semiconductor, the intensity of the light drops exponentially as the photons are converted to electron-hole paires by the process of "photogeneration":

$$I = I_0 e^{-\alpha x} \tag{2.2}$$

where α is the absorption coefficient typically in cm^{-1}, and x is the distance into the material. I_0 is the light intensity just inside the surface of the semiconductor. Since each photon absorbed generates an e-h pair, this exponential decay also mimics the generation of carriers as a function of depth.

The generation rate, G, is given by:

$$G = \alpha N_0 e^{-\alpha x} \tag{2.3}$$

where N_0 is the photon flux at the surface (photons/unit-area/sec), α is absorption coefficient, and x is the distance into the material. Generation occurs in PV cells by absorption of light, and

the formation of electron-hole pairs. The absorption coefficient α in units of cm^{-1}, provides a measure of the strength of the light absorption at a given photon energy [5].

The optical absorption coefficient α is given by:

$$\alpha = \frac{4\pi k}{\lambda} \tag{2.4}$$

Figure 2.2 gives the absorption spectra of some materials. The minimum energy required for the incident photon to cause the electronic transition depends on the band gap E_g of the material.

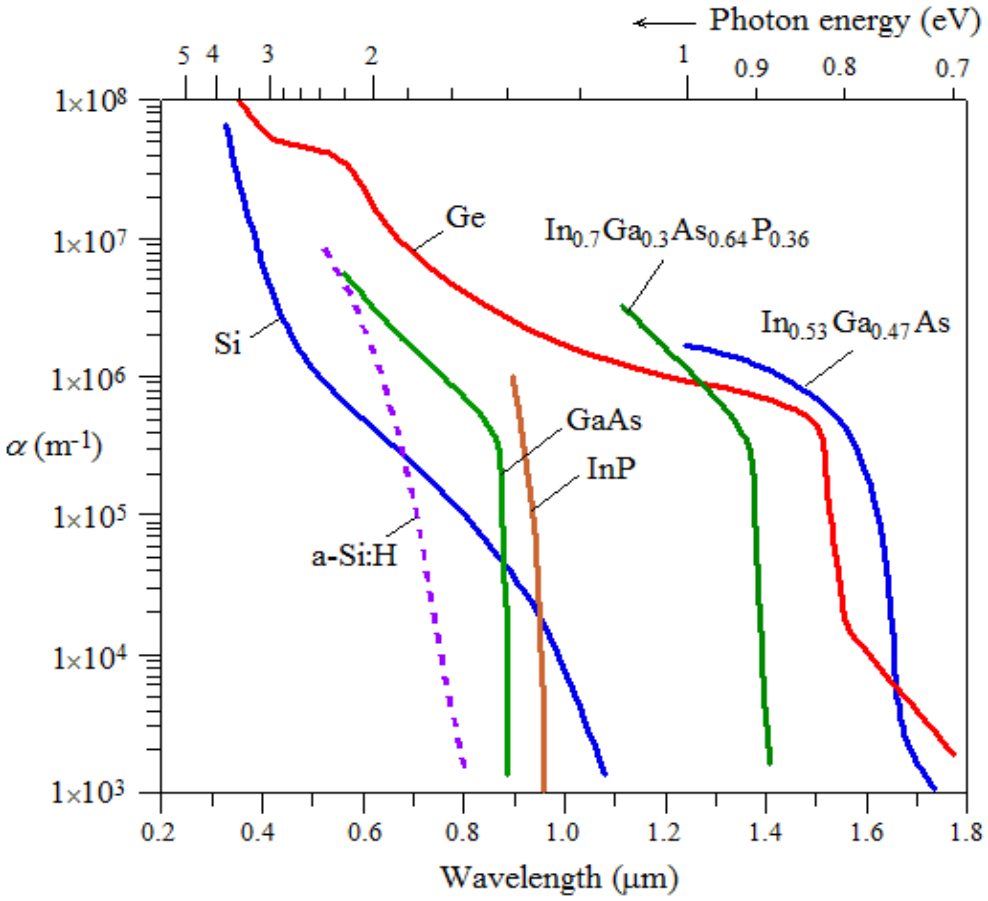

Figure 2.2 Absorption coefficient as a function of wavelength of light (bottom abscissa) or energy (top abscissa) for several semiconductors [6].

2.5 How a Solar Cell Works

A solar cell is made from two types of silicon semiconductors: p-type and n-type.

P-type silicon is created by adding elements like boron or gallium to pure silicon. These elements have one less electron in their outer shell than silicon. Because of this, when boron bonds with silicon atoms, it leaves behind an electron vacancy, known as a "hole."

N-type silicon, in contrast, is made by adding elements such as phosphorus, which have one more electron in their outer shell than silicon. Phosphorus forms bonds with surrounding silicon atoms, but its extra electron doesn't participate in bonding. Instead, it remains free to move, making the material a good conductor of electricity.

In a solar cell, a layer of p-type silicon is placed next to a layer of n-type silicon (see Figure2.3). The n-type layer has extra electrons, while the p-type layer has extra holes. At the junction between these layers, some electrons from the n-type side move into holes on the p-type side, creating a narrow region called the depletion zone**.** Here, the electrons fill the holes, effectively canceling out the charge in that area [7].

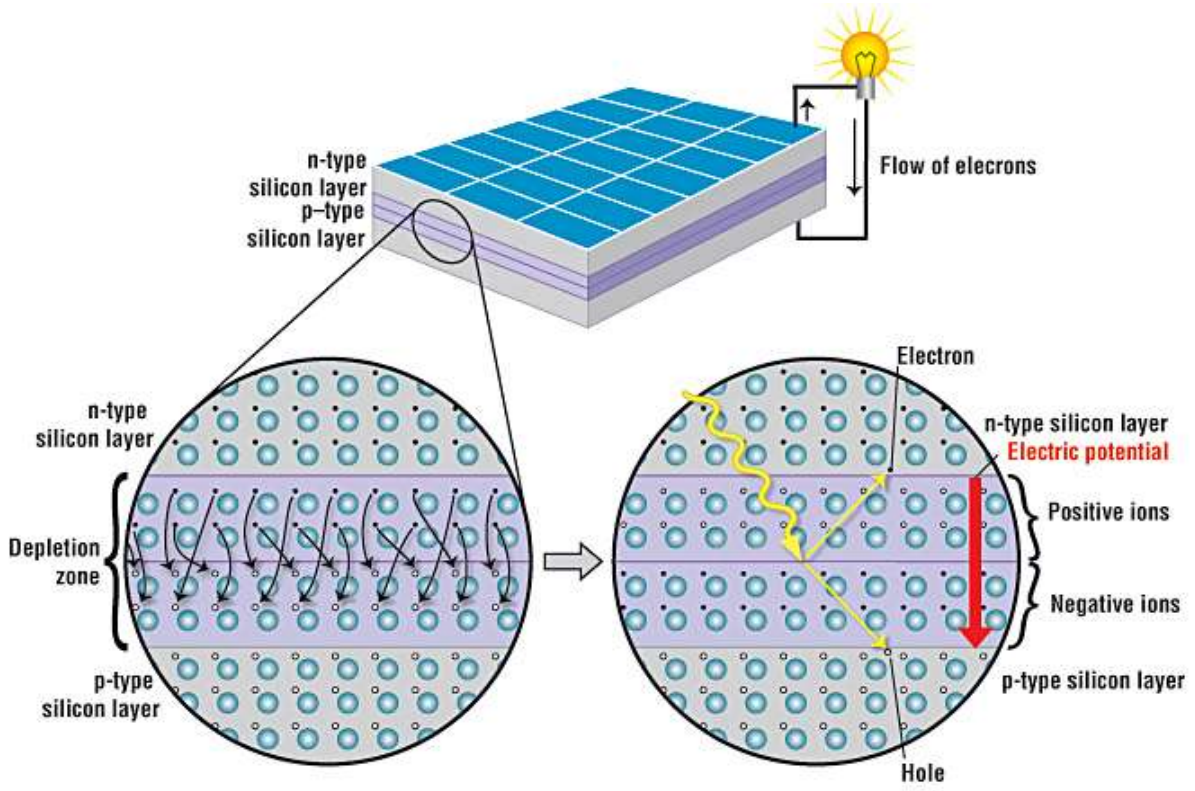

Figure 2.3 Schematic representation of a solar cell, showing the n-type and p-type layers, with a close-up view of the depletion zone around the junction between the n-type and p-type layers.

As a result, the p-type side of the depletion zone becomes negatively charged, and the n-type side becomes positively charged, forming an electric field. This internal electric field acts as a barrier—it prevents further movement of electrons across the junction.

When sunlight hits the solar cell, it gives energy to electrons in the silicon, causing them to break free from their atoms. This leaves behind new holes. If this happens within the depletion zone, the electric field pushes the freed electrons toward the n-type layer and the holes toward the p-type layer.

If the two layers are connected by a metal wire, the electrons will flow through the wire from the n-type layer to the p-type layer, where they recombine with holes. This flow of electrons through the external circuit produces electric current, which can be used to power electrical devices [7].

2.6 Electrical characteristics

2.6.1 The ideal solar cell

An ideal solar cell can be represented by a current source connected in parallel with a rectifying diode, as shown in the equivalent circuit of Figure 2.4. The corresponding *I–V* characteristic is described by the Shockley solar cell equation:

$$I = I_{ph} - I_0\left(e^{\frac{qV}{k_B T}} - 1\right) \tag{2.5}$$

where k_B is the Boltzmann constant, T is the absolute temperature, q is the electron charge, and V is the voltage at the terminals of the cell. I_o is the diode saturation current. The photogenerated current I_{ph} is closely related to the photon flux incident on the cell, and its dependence on the wavelength of light is frequently discussed in terms of the quantum efficiency or spectral response.

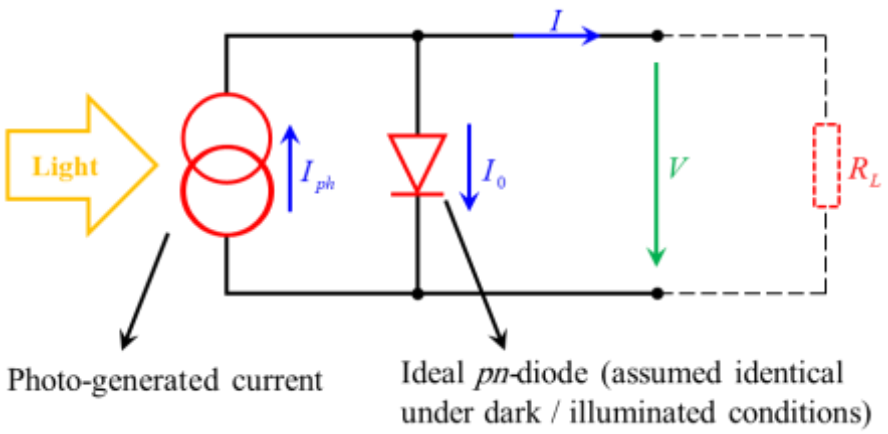

Figure 2.4 Simplest equivalent circuit, for an "ideal" solar cell; an external load resistance R_L has also been drawn.

Figure 2.5(a) shows the *I–V* characteristic (Equation (2.5)). In the ideal case, the short-circuit current I_{sc} is equal to the photogenerated current I_{ph}, and the open-circuit voltage V_{oc} is given by

$$V_{OC} = \frac{k_B T}{q} \ln\left(1 + \frac{I_{ph}}{I_0}\right) \tag{2.6}$$

The power $P=IV$ produced by the cell is shown in Figure 2.5(b). The cell generates the maximum power P_{max} at a voltage V_m and current I_m, and it is convenient to define the fill factor *FF* by:

$$FF = \frac{I_m V_m}{I_{sc} V_{oc}} = \frac{P_{\max}}{I_{sc} V_{oc}} \tag{2.7}$$

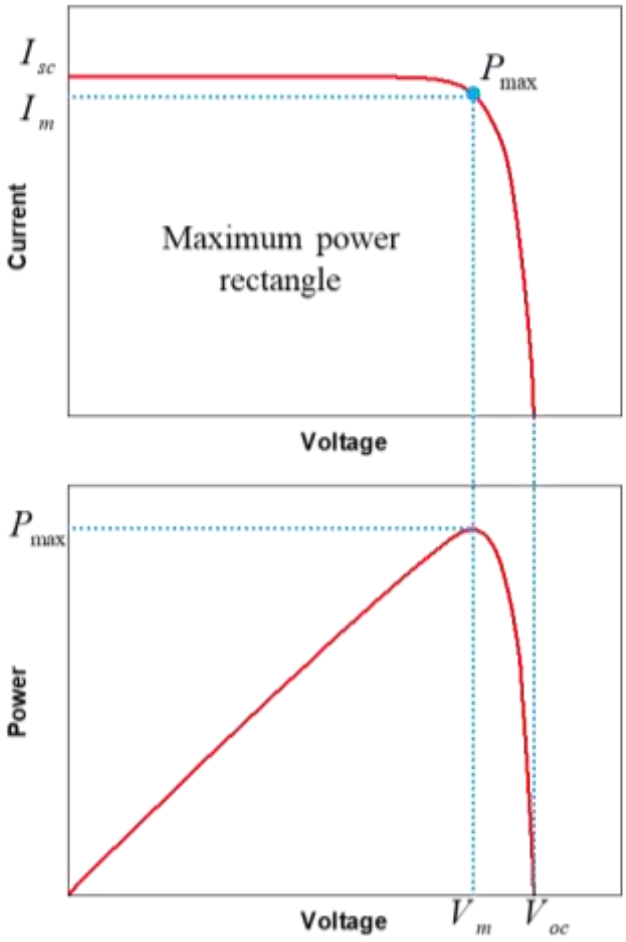

Figure 2.5 (a) The *I–V* characteristic of an ideal solar cell and (b) the power produced by the cell. The power generated at the maximum power point is equal to the shaded rectangle in (a).

The fill factor *FF* of a solar cell with the ideal characteristic (2.5) will be furnished by the subscript 0. It cannot be determined analytically but it can be shown that FF_o depends only on the ratio $v_{oc} = V_{oc} / k_B T$. FF_o is determined by the approximate expression.

$$FF_o = \frac{v_{oc} - \ln(v_{oc} + 0.72)}{v_{oc} + 1} \tag{2.8}$$

The efficiency η, of solar cells refers to the power conversion efficiency. It is defined as the ratio between the maximum power delivered by the cell and the incident light power P_{in}

$$\eta = \frac{P_m}{P_{in}} = \frac{FFV_{co}I_{cc}}{P_{in}} \tag{2.9}$$

P_{in} : the incident light power is equal to the solar power P_{solar} (P_{solar}= 100 mW/cm^2).

The *I–V* characteristics of an ideal solar cell complies with the *superposition principle:* the functional dependence (2.5) can be obtained from the corresponding characteristic of a diode in the dark by shifting the diode characteristic along the current axis by I_{ph} (Figure 2.6).

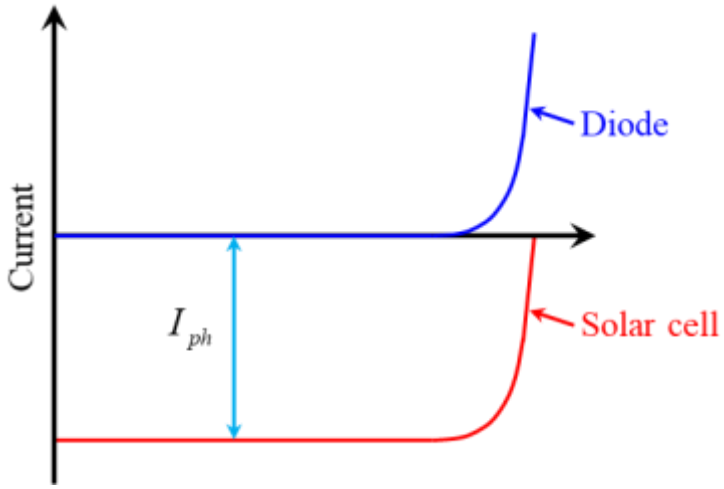

Figure 2.6 The superposition principle for solar cells.

2.6.2 Solar cell characteristics in practice

The *I–V* characteristic of a solar cell in practice usually differs to some extent from the ideal characteristic eq. (2.5). The solar cell (or circuit) may also contain series (R_s) and parallel (or shunt, R_p) resistances, leading to a characteristic of the form:

$$I = I_{ph} - I_0\left\{\exp\left(\frac{V + IR_s}{2k_BT}\right) - 1\right\} - \frac{V + IR_s}{R_p} \tag{2.11}$$

where the light-generated current I_{ph} may, in some instances, depend on the voltage. These features are shown in the equivalent circuit of Figure 2.7. The effect of the series and parallel resistances on the *I–V* characteristic of the solar cell is shown in Figures 2.8. The effect of the series resistance on the fill factor can be writing as [8, 9]:

$$FF = FF_o(1 - r_s) \tag{2.12}$$

where $r_s = R_sI_{sc}/V_{oc}$. An analogous expression exists also for the parallel resistance.

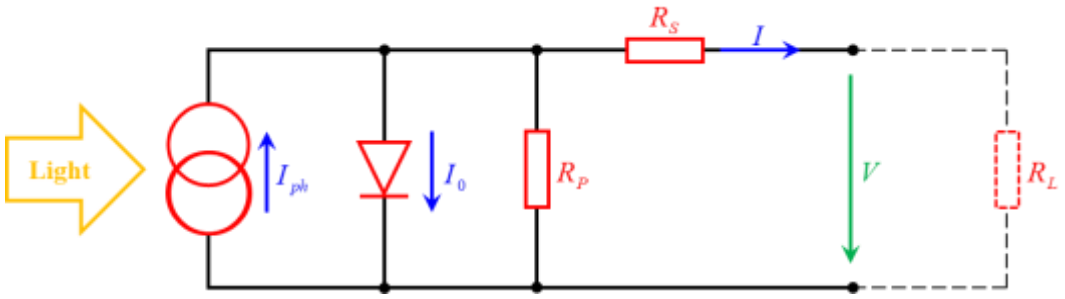

Figure 2.7 Universally used equivalent circuit for a solar cell.

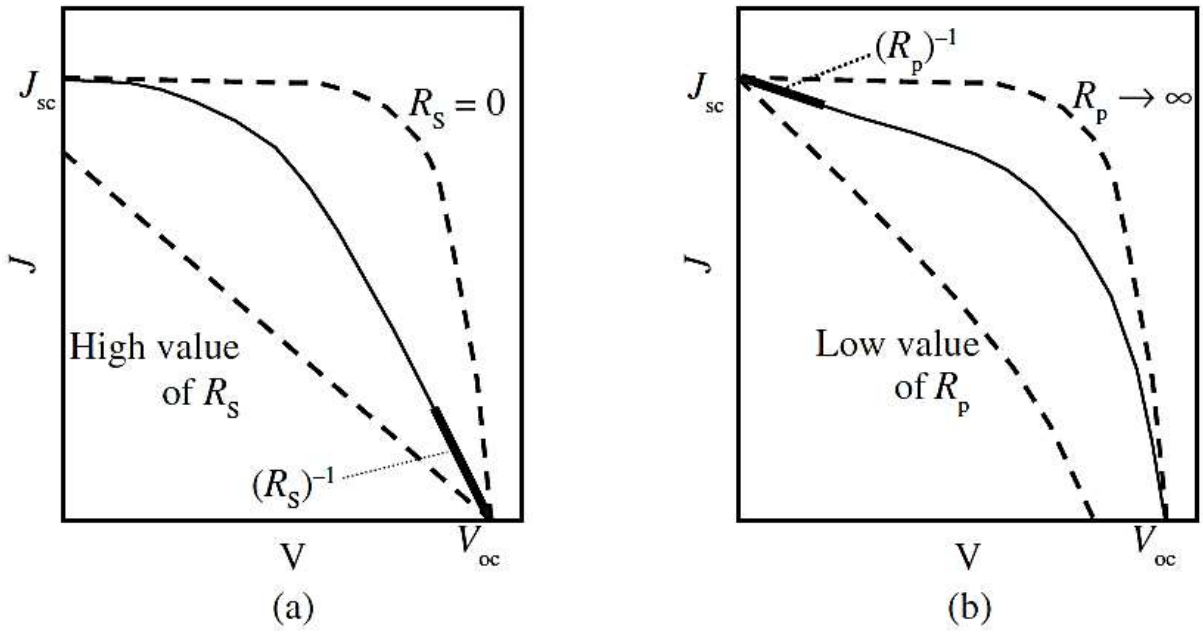

Figure 2.8 Effect of (a) the series resistance R_s and of (b) the parallel resistance R_p, as given in the "universal" circuit of Fig. 2.13 on the $J(V)$ characteristics of a solar cell. Values of $(R_s)^{-1}$ and $(R_p)^{-1}$ are given by the slopes of the $J(V)$ characteristics, at the short-circuit point ($V = 0$) and at the open-circuit point ($J = 0$), respectively.

2.7 Types of Solar Cells

- **First generation (crystalline)**

First-generation solar panels are the most used PV technology and have been around since solar energy's earliest days.

First-generation solar panels utilise traditional crystalline silicon technology. This comes in two types – monocrystalline and polycrystalline – based on the manufacturing process.

- **Second generation (thin film)**

Second-generation solar panels emerged after the crystalline silicon type. Characterised by their use of alternative manufacturing processes and semiconductor materials, the second generation includes thin film, dye-sensitised and organic solar panels.

Most solar panels from the second generation rely on thin-film solar cell technology. Thin-film solar cells are made with multiple layers of PV material on top of a substrate, such as cadmium, copper or silicon.

❖ **Third generation**

Third-generation solar panels represent the next phase of innovation and development in solar PV technology. Third-generation panels – which include perovskite, tandem and multijunction varieties – are defined by a focus on advanced materials, novel designs and fresh concepts to refine energy efficiency, boost cost effectiveness and improve sustainability.

There are totally seven different types of solar panels available in 2024:

- First generation – crystalline
    - Monocrystalline
    - Polycrystalline
- Second generation – thin film
    - Silicon – a-Si
- Third generation
    - Dye-sensitised solar cells (DSSCs)
    - Organic
    - Perovskite
    - Concentrated photovoltaic (PV) cell – concentrated PV (CVP) and highly concentrated PV (HCPV)
- Cutting edge and future technology
    - Heterojunction technology (HJT)
    - Bifacial cells
    - Half-cut cell or cut cell
    - Shingled solar cells

2.8 Conclusion

In conclusion, understanding the fundamentals of solar cell devices lays the groundwork for advancements in photovoltaic technology. This chapter has explored the basic principles governing solar cell operation, including the photovoltaic effect, the structure and materials used, and key performance parameters such as efficiency, fill factor, and open-circuit voltage.

By grasping these core concepts, one can better appreciate the challenges and innovations in solar energy conversion. As research progresses, the continued refinement of solar cell design and materials holds great promise for meeting the world's growing energy needs sustainably.

Chapter 2 references

[1] *Solar Radiation Basics*. (n.d.). Energy.gov. https://www.energy.gov/eere/solar/solar-radiation-basics

[2] S. M. Sze and M. K. Lee, "Semiconductor devices: phys-ics and technology. 3-rd edition.-New York, John Wiley and Sons, Inc," 2012.

[3] Administrator. (n.d.). *Photovoltaic Solar Cell Turns Photons into Electrons Using Semiconductors*. Alternative Energy Tutorials. https://www.alternative-energy-tutorials.com/photovoltaics/photovoltaics-turn-photons-into-electrons.html

[4] H. Mathieu and H. Fanet, *Physique des semiconducteurs et des composants électroniques-6ème édition: Cours et exercices corrigés*. Dunod, 2009.

[5] GENERATION AND RECOMBINATION OF CHARGE CARRIERS IN SOLAR CELLS; TRANSPORT MECHANISMS: DRIFT AND DIFFUSION. (2012). In University of Toledo.

[6] G. Barbarino, F. Barbato, and E. Nocerino, "The Semiconductor Multiplication System for Photoelectrons in a Vacuum Silicon Photomultiplier Tube (VSiPMT) and Related Front End Electronics."

[7] *How a solar cell works - American Chemical Society*. (n.d.-b). American Chemical Society. https://www.acs.org/education/chemmatters/past-issues/archive-2013-2014/how-a-solar-cell-works.html

[8] Kateb Mohamed Nadjib, "Numerical simulation study of a-Si:H/µc-Si:H multijunction solar cell", Phd thesis, Biskra University, 2022.

[9] T. Markvart, A. McEvoy, and L. Castaner, Practical handbook of photovoltaics: fundamentals and applications. Elsevier, 2003.

[10] *Types of solar cells explained*. (2024, March 19). Federation of Master Builders. https://Https://www.fmb.org.uk/homepicks/solar-panels/types-of-solar-cells/

Chapter 3:

SCAPS-1D program and simulation

3.1 Introduction

The growing need for renewable and sustainable energy sources has led to increased interest in advanced photovoltaic technologies. Among the materials investigated for high-performance solar cells, InGaP stands out due to its favorable electronic and optical properties. It is especially relevant in high-efficiency and multi-junction solar cell applications.

This chapter presents a detailed simulation study of solar cells incorporating InGaP material using SCAPS-1D software. The objective is to analyze and optimize the performance of InGaP-based devices by adjusting key parameters and observing their impact on solar cell characteristics.

The chapter outlines the modeling process, simulation settings, and results, focusing on efficiency, current-voltage behavior, and other performance metrics. Through this work, we aim to provide insight into the potential of InGaP as an absorber layer and demonstrate the effectiveness of SCAPS in simulating its behavior in photovoltaic structures.

3.2 Definition and Overview of SCAPS Logiciel (SCAPS-1D)

3.2.1 What is SCAPS?

SCAPS-1D (*Solar Cell Capacitance Simulator*) is a numerical simulation software developed by the University of Ghent, Belgium, specifically designed for analyzing the performance of layered semiconductor structures in solar cells. The software models the electrical and optical behavior of one-dimensional thin-film solar cells, considering both steady-state and transient conditions.

SCAPS helps researchers simulate and optimize the physical behavior of solar cell devices, especially those based on:

- CdTe (Cadmium Telluride)
- CIGS (Copper Indium Gallium Selenide)
- CZTS (Copper Zinc Tin Sulfide/Selenide)
- Perovskite materials
- Silicon-based devices

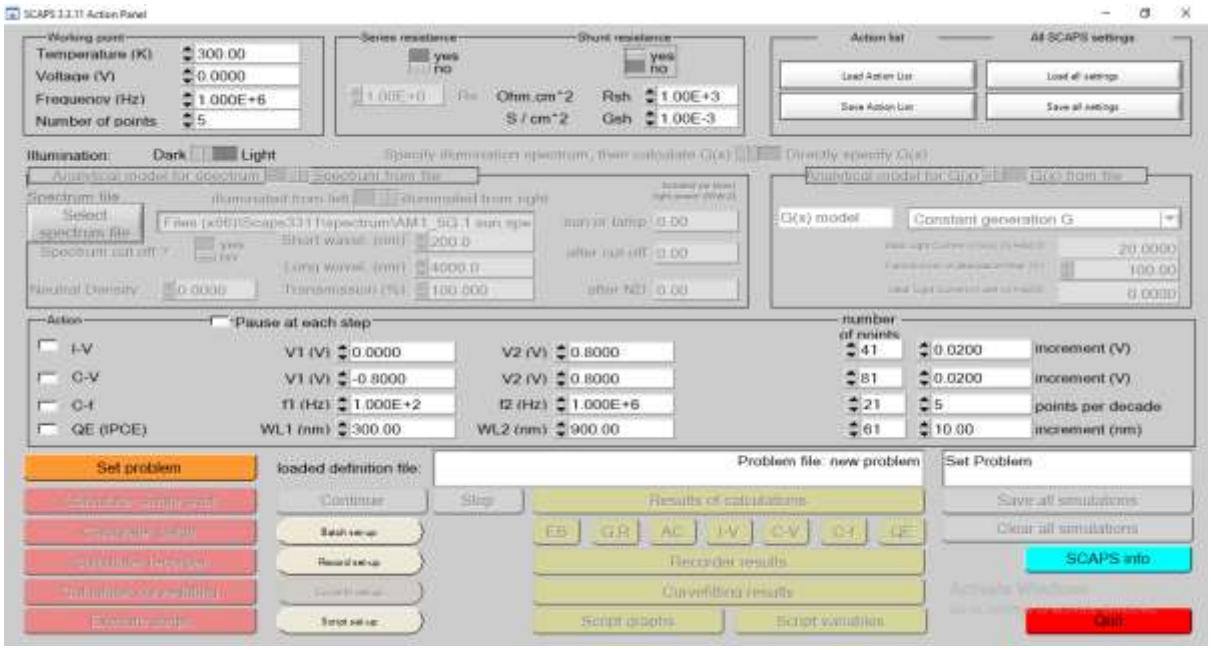

Figure 3.1: SCAPS the Action panel or main panel

3.2.2. Simulation Capabilities

SCAPS is capable of modeling:

- Electrical characteristics:
  - Current-Voltage (J-V) curves under dark and illuminated conditions
  - Capacitance-Voltage (C-V) behavior
  - Quantum Efficiency (QE) and External Quantum Efficiency (EQE)
  - Admittance and transient simulations (e.g., impedance spectroscopy)
- Physical mechanisms:
  - Charge carrier transport (drift and diffusion)
  - Recombination (Shockley-Read-Hall, surface, tunneling)
  - Generation under light
  - Influence of defect levels, interface states, and band alignment
- Device structure:
  - Up to 7 different semiconductor layers
  - Each with individual band gaps, doping concentrations, mobility, permittivity, and more
  - Inclusion of buffer, absorber, window, back contact, front contact layers, etc.

3.2.3. Equations and Numerical Approach

SCAPS solves the basic semiconductor equations:

- Poisson's equation (for electrostatic potential)
- Electron continuity equation
- Hole continuity equation

These equations are solved using a finite-difference discretization method in one dimension (1D), under both equilibrium and non-equilibrium (illumination, bias voltage) conditions.

3.2.4. Application and Importance

SCAPS is widely used in research to:

- Optimize material parameters (bandgap, doping, mobility)
- Study defects and trap states
- Investigate the effect of interface quality
- Analyze heterojunction performance
- Design new solar cell architectures (e.g., perovskite/silicon tandem cells)

It is particularly useful for predictive modeling, device optimization, and experimental result validation in photovoltaic R&D.

3.2.5. System Requirements and Accessibility

- SCAPS is a Windows-based standalone application.
- It is free for academic use, provided by the ELIS department of Ghent University [1].

3.3 InGaP solar cell

The InGaP solar cell (Indium Gallium Phosphide) is a type of III-V semiconductor solar cell known for its high efficiency and widespread use in advanced and space applications. InGaP is composed of a mixture of indium, gallium, and phosphorus, and its bandgap can be tuned by adjusting the ratios of these elements to suit specific applications and to ensure lattice matching with other layers. InGaP solar cells are typically used as the top cell in multi-junction solar cells, where their wide bandgap allows them to efficiently capture high-energy photons. Using single junction with two types cell,

the first cell we used n-p InGaP (n-InGaP, P-InGaP), and for the second cell we used n-n-p (n-InGaP,n-Ge,p-Ge), we reched to efficiency of 22.21% for the first cell and 13.26 % of the second solar cell.

3.4 Device structure of n-p InGaP solar cell and simulation parameters

Figure 3.2 presents the structure of a n-p InGaP solar cell, with the physical parameters used in the numerical simulation listed in Table 3.1. This structure features n-InGaP and p-InGaP layers.

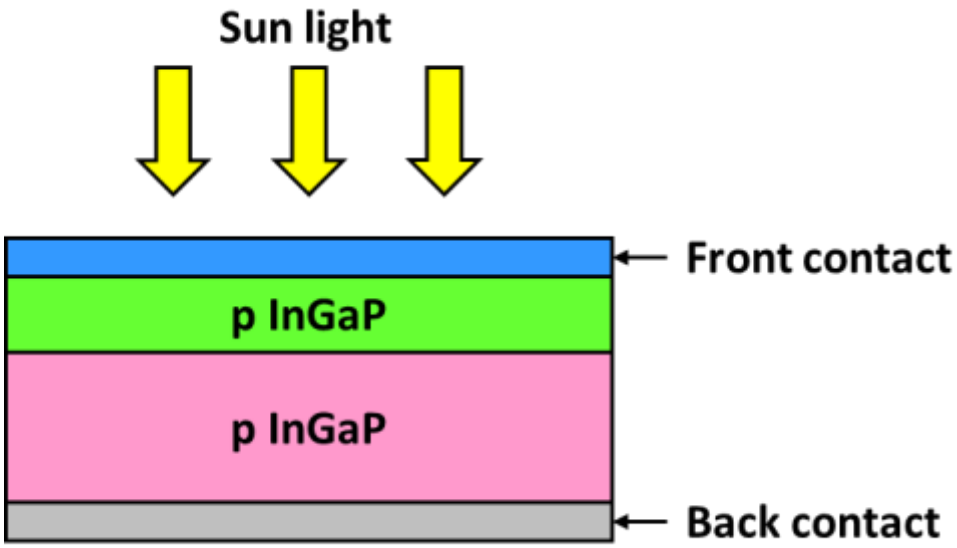

Figure 3.2 Schematic diagram of n-p InGaP solar cell.

Parameters	**InGaP**
Band Gap Energy (eV)	1.61
Band Gap Energy (eV)	**5.65**
Dielectric permittivity	**11.6**
Affinity (eV)	**4.16**
Effective Density of States in Conduction Band (per cc)	**1.3×10^{20}**
Effective Density of States in Valence Band (per cc)	**1.28×10^{19}**
Electron Mobility (cm2/Vs)	**1945**
Holes Mobility (cm2/Vs)	**141**

Table 3.1 Geometric and physical parameters set for simulation of the n-p InGaP solar cell [2].

3.5 solar cell performance

The first simulation step consists of the simulation of InGaP based n p solar cell. The parameter values adopted in the simulation are given in Tables.

Simulation studies are carried out using an InGaP structure consisting of front contact/n-InGaP (1µm)/ p-InGaP (1µm)/backcontact which is shown in

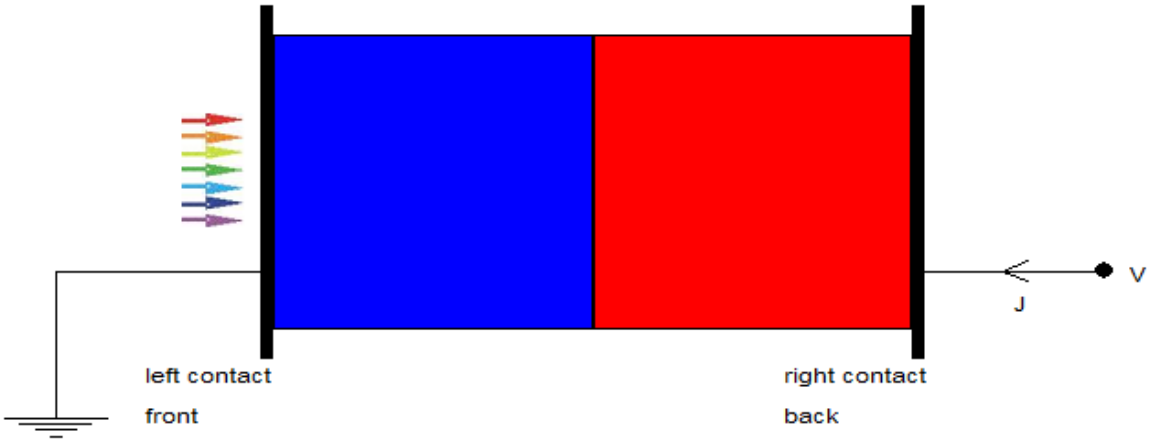

Figure 3.3 Simulated structure of a np InGaP solar cell in SCAPS.

The J–V characteristic simulated for InGaP solar cell is presented in. Table 3.2 shows the photo electrical parameters of InGaP solar cell extracted from the corresponding J–V characteristic.

	J_{sc}(mA/cm^2)	V_{oc}(V)	*FF* (%)	η (%)
InGaP cell simulation	5.77	0.93	84.2	4.51

Table 3.2 Simulation and photovoltaic parameters of InGaP solar cell.

The electrical characteristics of the InGaP solar cell obtained through simulation are, respectively, *Jsc*=5.77mA/cm2, *Voc*=0.93 V, *FF*=84.2%, η=4.51 % .

3.6 Optimization of InGaP solar cell performance

In a second stage, we improved the performance of the solar cell by:

- Optimization of thicknesses of solar cell layers.
- Optimization of acceptor and donor concentrations of p layer and n layer respectively.

3.6.1 Optimization of thicknesses of solar cell InGaP layers

a) n layer

Many simulations are executed with the variations of the thicknesses from 10 nm to 100 nm of n-layer (Fig. 3.4). However, with the increasing of thicknesses, the efficiency η increased from 4.51 % to 16.52 % in thicknesses of 40nm. The results indicate that the thicknesses enhance the efficiency. The n-layer thicknesses of 40 nm considered an optimized value.

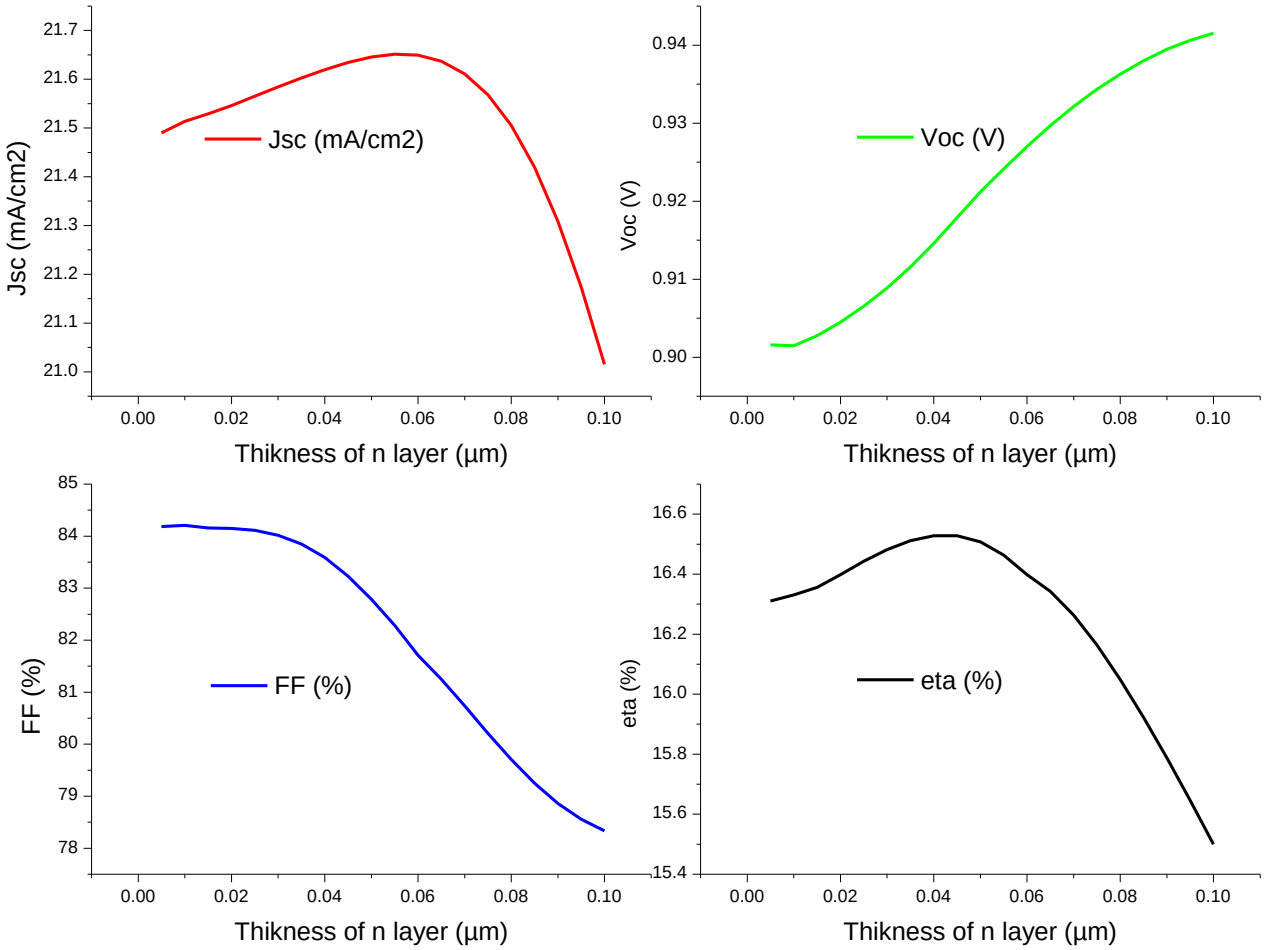

Figure 3.5 Simulated photovoltaic parameters of InGaP solar cell as function of thickness of the n-layer

b) p layer

As shown in Fig.3.6, with increasing n layer thickness from 1 µm to 200 µm, the efficiency η increased from 16.52 %. To 19.91% at the p-layer thickness of 126 µm. The p-layer thickness of 126 µm considered an optimized value.

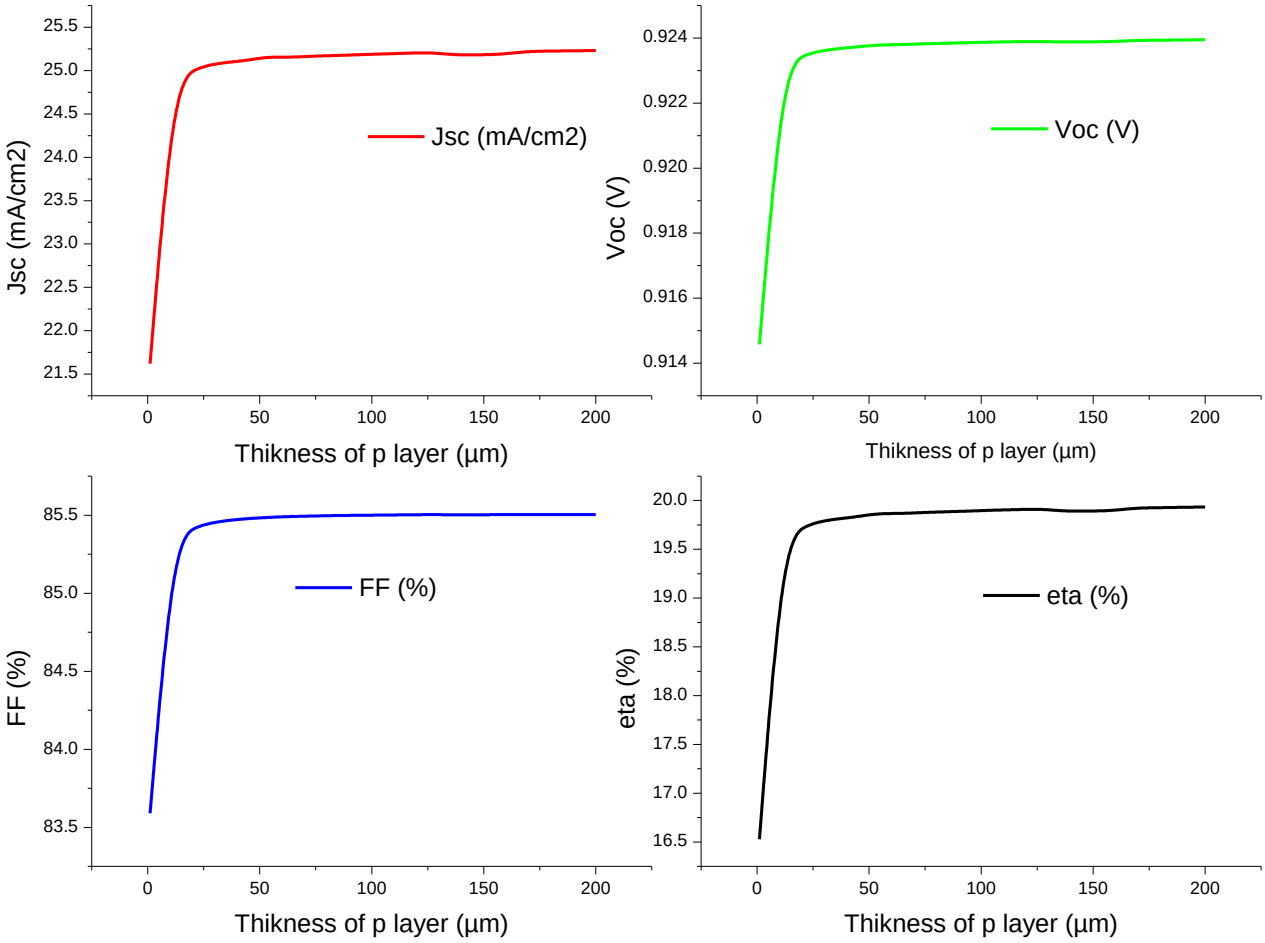

Figure 3.6 Simulated photovoltaic parameters of InGaP solar cell as function of thickness of the p-layer

3.6.2 Optimization of concentrations of solar cell layers

a) donor concentrations

Once we obtained optimal thicknesses by simulation, we performed optimizing the concentrations on the photoelectrical parameters of InGap solar cell, in view of this, we have also examined the behaviours of J_{sc}, V_{oc}, FF and η as a function of concentrations of layers. As shown in Fig.3.7, with increasing N_D from $10^{17}cm^{-3}$to $10^{19}cm^{-3}$of n-layer. η has a maximum value of 21.61% at N_D of $10^{19}cm^{-3}$ µm.

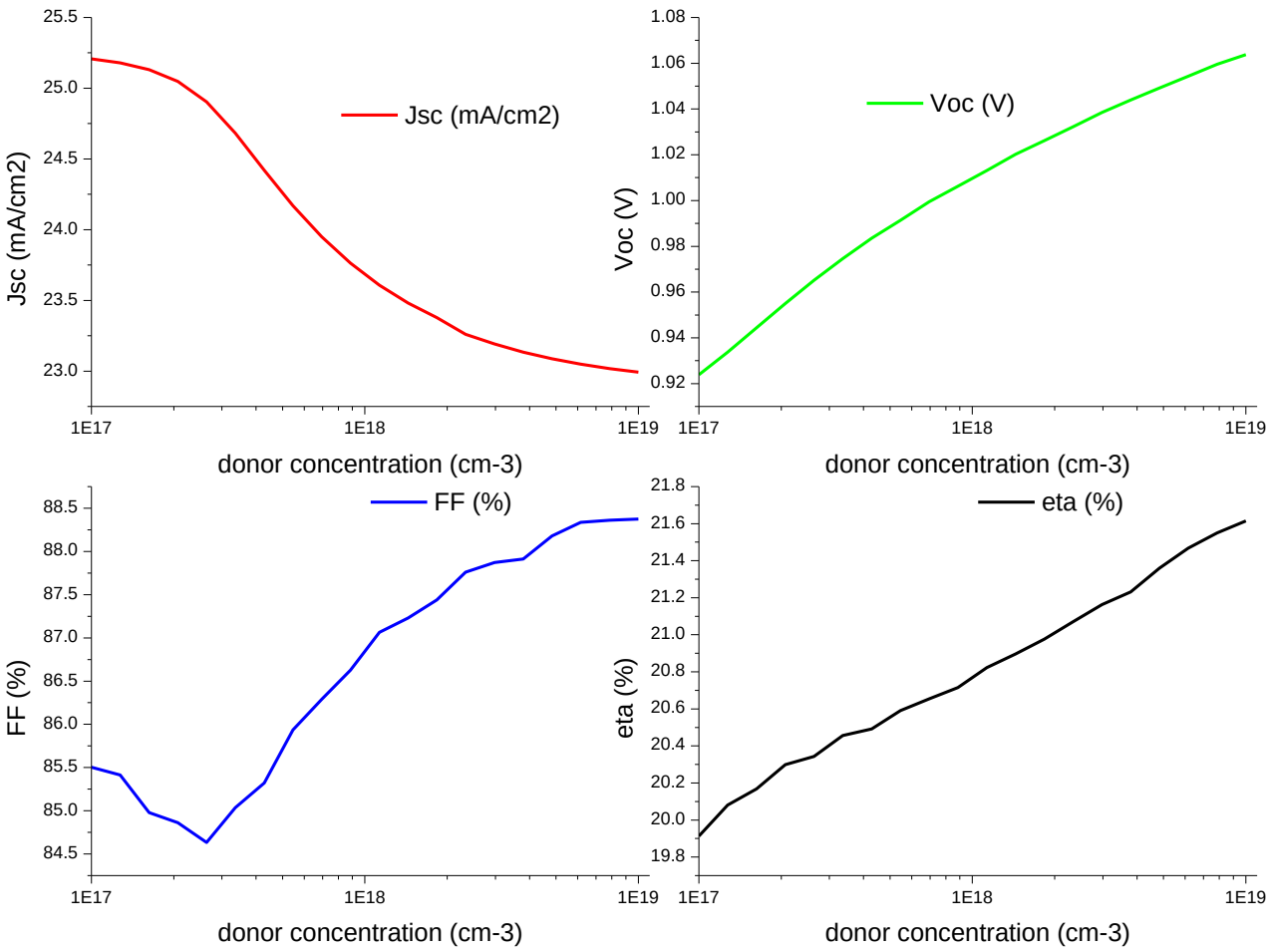

Figure 3.7 Simulated photovoltaic parameters of InGaP solar cell as function of donor concentrations of the n-layer

b) acceptor concentrations

The simulations are executed with the variations of the acceptor concentration N_A from 10^{17} cm^{-3} to 10^{19} cm^{-3} of p-layer (Fig. 3.8). However, with the increasing of N_A, the efficiency η increased from 21.61 % to 22.21 %. The results indicate that the dopant concentration N_A enhances the efficiency. The p-layer concentration of 10^{19} cm^{-3} considered an optimized value.

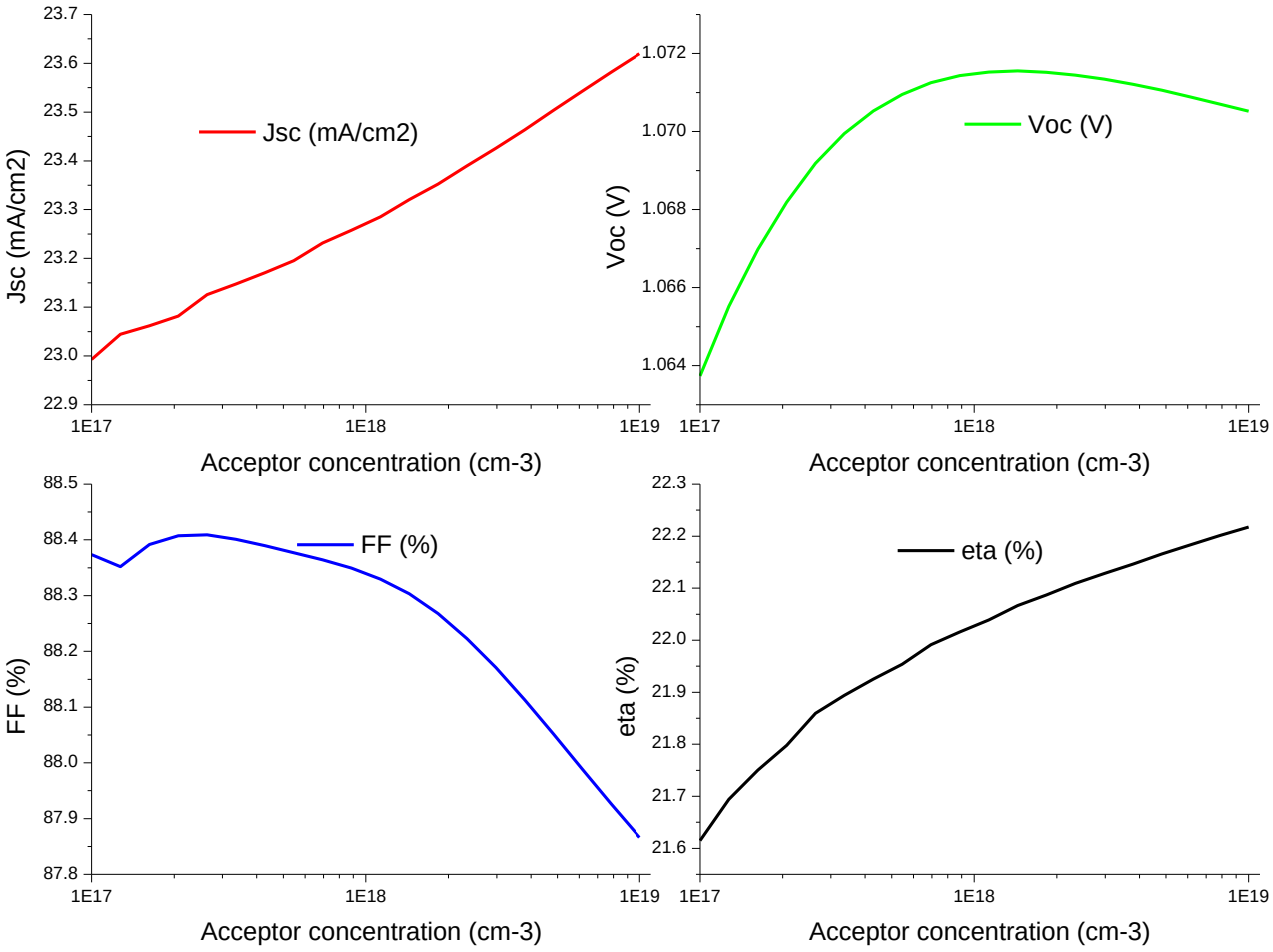

Figure 3.8 Simulated photovoltaic parameters of InGaP solar cell as function of acceptor concentrations of the p-layer

After improvement of J–V characteristic of InGaP solar cell by optimization of thicknesses of solar cell n, and p layers and optimization of donor and acceptor concentrations of n layer and p layer. Table 3.3 shows the photo electrical parameters of optimized InGaP solar cell extracted from the corresponding J–V characteristic.

The electrical characteristics of the optimized InGaP solar cell obtained through simulation are, respectively, *Jsc*=23.61 mA/cm^2, *Voc*=1.07 V, *FF*=87.86 %, η=22.21 %.

	J_{sc}(mA/cm^2)	V_{oc}(V)	*FF* (%)	η (%)
InGaP cell simulation	23.61	1.07	87.86	22.21

Table 3.3 Simulation and photovoltaic parameters of optimized InGaP solar cell.

3.7 Device structure of InGaP/Ge solar cell and simulation parameters

Figure 3.9 presents the structure of a p-n-n InGaP/Ge solar cell, with the physical parameters used in the numerical simulation listed in Table 3.4. This structure features p-InGaP and n-Ge , p-Ge layers. The n-n-p configuration creates an electric field between the p and n regions, which efficiently separates electron-hole pairs and minimizes recombination. When light is absorbed, electrons are excited from the valence band to the conduction band, leaving behind holes in the valence band. These charge carriers move through the material, contributing to the generation of photocurrent.

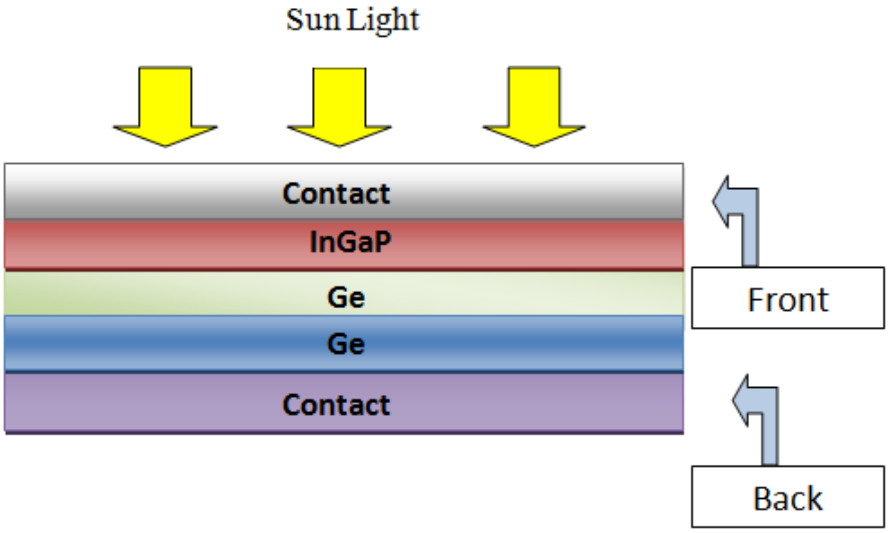

Figure 3.9 The structure of n-n-p InGaP/Ge solar cell

Parameters	**InGaP**	**Ge**
Band Gap Energy (eV)	1.61	**0.66**
Band Gap Energy (eV)	**5.65**	**5.64**
Dielectric permittivity	**11.6**	**16**
Affinity (eV)	**4.16**	**16**
Effective Density of States in Conduction Band (per cc)	**$1.3x10^{20}$**	**$1.04x10^{19}$**
Effective Density of States in Valence Band (per cc)	**$1.28x10^{19}$**	**$6x10^{18}$**
Electron Mobility (cm2/Vs)	**1945**	**3900**
Holes Mobility (cm2/Vs)	**141**	**1900**

Table 3.4 Parameters set for simulation of the InGaP/Ge solar cell [2]

3.8 solar cell performance

The first simulation step consists of the simulation of InGaP/Ge based n-n-p solar cell. The parameter values adopted in the simulation are given in Tables 3.4

Simulation studies are carried out using an InGaP/Ge structure consisting of frontcontact/n-InGaP (200nm)/n-Ge (200 nm)/p-Ge (200 nm)/backcontact which is shown in

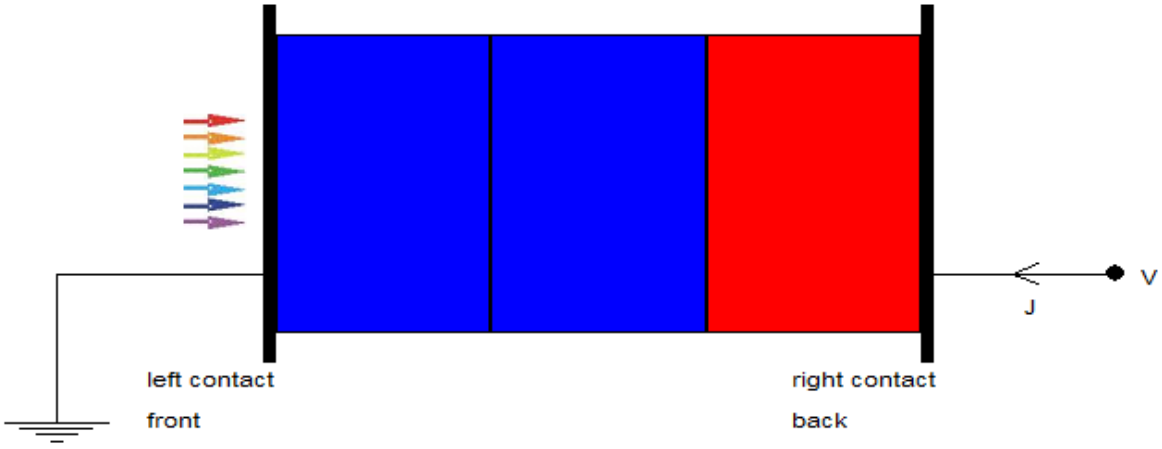

Figure 3.10 Simulated structure of a np InGaP/Ge solar cell in SCAPS.

The J–V characteristic simulated for InGaP/Ge solar cell is presented in. Table 3.5 shows the photo electrical parameters of InGaP/Ge solar cell extracted from the corresponding J–V characteristic.

	J_{sc}(mA/cm^2)	V_{oc}(V)	*FF* (%)	η (%)
InGaP/Ge cell simulation	35.66	0.11	50.19	2.05

Table 3.5 Simulation and photovoltaic parameters of InGaP/Ge solar cell.

The electrical characteristics of the InGaP/Ge solar cell obtained through simulation are, respectively, *Jsc*=35.66 mA/cm2, *Voc*=0.11 V, *FF*=50.19 %, η=2.05 % .

3.9 Optimization of InGaP solar cell performance

In a second stage, we improved the performance of the solar cell by:

- Optimization of thicknesses of solar cell layers.
- Optimization of acceptor and donor concentrations of p layer and n layer respectively.

After improvement of J–V characteristic of InGaP/Ge solar cell by Optimization of acceptor and donor concentrations of p layer and n layer respectively and optimization of thicknesses of solar cell p and n layers. Table 3.6 shows the photo electrical parameters of optimized InGaP/Ge solar cell extracted from the corresponding J–V characteristic.

The electrical characteristics of the optimized InGpa solar cell obtained through simulation are, respectively, Jsc=60.81 mA/cm^2,Voc=0.3018 V, FF=72.26 %, η=13.26 %.

	J_{sc}(mA/cm^2)	V_{oc}(V)	FF (%)	η (%)
InGaP/Ge cell simulation	60.81	0.30	72.26	13.26

Table 3.6 Simulation and photovoltaic parameters of optimized InGaP/Ge solar cell.

3.10Conclusion

This chapter demonstrated the capability of SCAPS-1D in simulating and optimizing InGaP-based solar cells. Initial simulations showed modest efficiency, but through systematic optimization of layer thicknesses and doping concentrations, a significant performance enhancement was achieved. The n-p InGaP cell reached an optimized efficiency of 22.21%, while the InGaP/Ge n-n-p cell achieved 13.26%. These results underline the importance of precise parameter tuning in photovoltaic design. SCAPS-1D proved to be an effective tool for performance analysis. Overall, InGaP remains a promising material for high-efficiency solar applications

Chapter 3 references

[1] Burgelman M, Decock K, Niemegeers A, et al. SCAPS manual most recent. Version 2021.

[2] Soley, S., & Dwivedi, A. (2021). Numerical simulation and performance analysis of InGaP, GaAs, Ge single junction and InGaP/GaAs/Ge triple junction solar cells. *Materials Today Proceedings*, *39*, 2050–2055. https://doi.org/10.1016/j.matpr.2020.11.056

General conclusion

In conclusion, this work provides a detailed exploration of photovoltaic principles, materials, and advanced simulation techniques for solar cell optimization. Beginning with the fundamental physics of solar energy conversion, the study established a clear understanding of key parameters influencing solar cell performance. The importance of material properties, particularly those of InGaP, was emphasized in achieving high-efficiency devices.

Using SCAPS-1D, a powerful numerical simulation tool, we modeled and analyzed various solar cell structures, focusing on n–p InGaP and n–n–p InGaP/Ge configurations. Through systematic optimization of layer thicknesses and doping concentrations, we demonstrated significant improvements in key performance indicators such as short-circuit current density (Jsc), open-circuit voltage (Voc), fill factor (FF), and overall efficiency (η).

The optimized n–p InGaP solar cell achieved an efficiency of 22.21%, while the n–n–p InGaP/Ge cell reached 13.26%. These results underline the critical role of simulation in guiding design choices and enhancing solar cell performance. SCAPS-1D proved to be a reliable and effective platform for predictive modeling, enabling better understanding and refinement of photovoltaic devices.

This study highlights the potential of InGaP-based technologies in the development of next-generation solar cells and supports continued research into multi-junction and high-efficiency photovoltaic systems.